JAERI-M
83-016

APPLICATION OF ENSDF DATA TO DECAY POWER AND GAMMA-RAY SPECTRUM CALCULATION

February 1983

Jun-ichi KATAKURA, Toshiharu HARA*
and Yoshitaka NAITO

日本原子力研究所
Japan Atomic Energy Research Institute

JAERI-M レポートは，日本原子力研究所が不定期に公刊している研究報告書です。
入手の問合わせは，日本原子力研究所技術情報部情報資料課（〒319—11 茨城県那珂郡東海村）あて，お申しこしください。なお，このほかに財団法人原子力弘済会資料センター（〒319-11 茨城県那珂郡東海村日本原子力研究所内）で複写による実費頒布をおこなっております。

JAERI-M reports are issued irregularly.
Inquiries about availability of the reports should be addressed to Information Section, Division of Technical Information, Japan Atomic Energy Research Institute, Tokai-mura, Naka-gun, Ibaraki-ken 319-11, Japan.

編集兼発行　日本原子力研究所
印　　刷　山田軽印刷所

JAERI-M 83-016

Application of ENSDF Data to Decay Power and Gamma-Ray Spectrum Calculation

Jun-ichi KATAKURA, Toshiharu HARA* and Yoshitaka NAITO

Division of Nuclear Safety Evaluation,
Tokai Research Establishment, JAERI

(Received January 26, 1983)

A decay data library was produced from the ENSDF (Evaluated Nuclear Structure Data File) for calculations of radioactive inventory, decay power or gamma-ray spectrum. In this report, the calculated results on the decay power and the gamma-ray spectra are shown and the applicability of the ENSDF is discussed. At short cooling times ($< 10^3$ sec), the results were underestimated for both decay power and gamma ray spectra. At long cooling times ($> 10^3$ sec), however, the calculated results were sufficiently acceptable. We also performed the calculation with the modified library (JDDL) in which the data for nuclides with no experimental informations were added and the insufficient data were replaced. Agreement with the experimental data was improved for decay power calculation at short cooling times.

Key words : Decay Data Library, Decay Power, Gamma-Ray Spectrum, Summation Calculation, Spectrum Calculation, ENSDF Data File

---

* I.S.L. Ltd.

JAERI-M 83-016

崩壊熱およびガンマ線スペクトル計算へのENSDFデータの適用

日本原子力研究所東海研究所安全解析部
片倉　純一・原　　俊治*・内藤　俶孝

（1983年1月26日受理）

評価済核構造データファイル（ENSDF：Evaluated Nuclear Structure Data File）から，放射性核種の生成量，崩壊熱，ガンマ線スペクトル計算用の崩壊データライブラリーを作成した。崩壊熱，ガンマ線スペクトルの計算を通してENSDFにおける崩壊データの適応性を検討した。冷却時間の短い所では（$< 10^3$ sec），崩壊熱・ガンマ線スペクトルとも実験値と比べて低目に算出されたが，冷却時間の長い所では（$> 10^3$ sec）充分満足出来る結果を得た。測定データが欠けているものや，不充分なデータしか与えられていない核種については，崩壊データを修正した。修正したライブラリー（JDDL）を用いることにより，短い冷却時間の所でも，崩壊熱に関しては，実験値と良い一致が得られた。

＊　アイ・エス・エル㈱

Contents

目　　次

1. Introduction

In safety evaluation of nuclear facilities, it is very important that build-up and depletion of nuclides, decay power, gamma- and beta-ray spectra are estimated accurately as sources in shielding or heat analysis. Nuclear decay data such as half-lives, Q-values, gamma-ray energies, gamma-ray intensities and so on are used in these calculations. These decay data are compiled in Table of Isotopes[1] or Nuclear Data Sheets[2]. Since the experimental data are increased year after year, nuclear structure and decay data were expected to be compiled in a computerized data file. Thus, the evaluation work for ENSDF (Evaluated Nuclear Structure Data File) has been developed under international cooperation[3]. It is a computerized file designed to draw up the tables or the drawings of Nuclear Data Sheets. The file is planned to be revised on a four-year cycle. The first cycle evaluation has not yet been completed, but we can now get the partly revised ENSDF twice a year. It will become the most reliable nuclear structure file in a few years, and it is now widely used in nuclear physics and other applied fields such as reactor physics.

In the present work, we produced a decay data library from the ENSDF of 1-81 version to calculate decay power and gamma-ray spectra to examine the ENSDF. We also performed the calculation with the modified library (JDDL) in which the nescessary data for nuclides with no experimental data and insufficient data were replaced by theoretically estimated ones. The calculated results were compared with the experimental results and the applicability of the ENSDF is discussed.

In section 2 the method to produce a decay data library from the ENSDF is given. The calculations of decay power and gamma-ray spectra are presented in section 3. The calculated results are given in section 4. The discussions about the calculated results are given in section 5.

2. Production of Decay Data Library

In the ENSDF, there are not only nuclear decay data set, but also nuclear reaction and adopted levels data sets. We can pick up most of the following data from nuclear decay data set in the ENSDF :

(1). Decay constants or half-lives,

(2). Q-values,

(3). decay types ($\beta^{\pm}$, α etc.),

(4). energy states (ground state or isomeric state),

(5). branching ratios of decay types,

(6). gamma-ray energies (including X rays),

(7). gamma-ray intensities,

(8). level energies,

(9). beta-ray energies (maximum energies),

(10). beta-ray intensities,

(11). beta decay types (allowed, first forbidden etc.),

(12). alpha-ray energies,

(13). alpha-ray intensities,

(14). internal conversion electron energies and

(15). internal conversion electron intensities.

Most of these data are directly obtained from the ENSDF, but X-ray data must be calculated by the gamma-ray intensity and the internal conversion coefficient together with other data such as X-ray fluorescence yield, specific X-ray energy and so on. They were taken from the data included in MEDLIST[4] , which is one of the utility codes of the ENSDF.

Only the X-rays following the emission of the internal conversion electrons were considered here, and X-rays following the electron capture were not, because such X-rays have small contributions to the decay power. In electron capture decay, the annihilation gamma rays due to positron emission were taken into account.

Intensities of K X-ray components (K_{α_1} , K_{α_2} and so on) are calculated by the following equation,

$$I_{KX_i} = f_K \cdot \omega_K \cdot N_{KX_i}$$

where f_K, ω_K, and N_{KX_i} are the number of the primary vacancies in the K-shell, the fluorescence yield in the K-shell and the probability of i component of K X-ray normalized to $\sum_i N_{KX_i} = 1.0$, respectively. Here, f_K is given by

$$f_K = I_\gamma \cdot \alpha_K ,$$

where I_γ is the absolute intensity of the gamma ray and α_K the internal conversion coefficient of K-shell.

In the case of the L-, M-, ···· X-rays, only the total intensities were calculated. The contributions of the secondary X rays following the production of the vacancies of the lower shells were also considered.

Another problem arises for the treatment of the isomeric state when the half-life of the parent nuclide is longer than or comparable with that of the isomeric state of the daughter nuclide. In this case, however, the gamma-ray intensities in the parent nuclide decay are given in equiliblium decay state. In calculating the decay power for short cooling time, the isomeric state should be considered to be different nuclide from the ground state. For this reason, it is needed to calculate the branching ratios to the isomeric state and to the ground state. Furthermore, the intensities of the gamma rays fed by the isomeric state must be subtracted from those in equiliblium state.

In Fig.1, X_i is the beta feeding ratio from the parent nuclide to the i-th level of the daughter nuclide and $T_{i\to j}$ the transition intensity ratio depopulating the i-th level to the j-th level. They are renormalised to be $\sum_i X_i = 1.0$ and $\sum_j T_{i\to j} = 1.0$. The branching ratio to the uppermost level of the daughter nuclide, level 6 in Fig.1, is expressed by the next equation,

$$P^6 = X_6 ,$$

and the next lower level, level 5 in Fig.1, is expressed by,

$$P^5 = X_5 + P^6 \cdot T_{6\to5} ,$$

and so on. Then the branching ratio to the isomeric state is

$$P^m = X_m + \sum_{i>m} P^i \cdot T_{i\to m} .$$

The branching ratio to the ground state is then

$$P^g = \sum_i X_i - P^m$$
$$= 1.0 - P^m .$$

When the decay scheme shown in left-hand side in Fig. 2 is given, the gamma rays from the isomeric state are contained in the parent nuclide decay. Therefore, the gamma rays fed by the isomeric state should be eliminated from the parent nuclide decay in the following way.

The energies and intensities of the gamma rays from the isomeric state are denoted as ${}^tE_i$ (${}^tE_0$, ${}^tE_1$ etc.) and ${}^tI_i$ (${}^tI_0$, ${}^tI_1$ etc.) as in right-hand side in Fig.2. These data are also included in the ENSDF as the decay data set of the isomeric transition. The energies and intensities of the gamma rays from the parent nuclide decay are denoted as ${}^pE_i$ (${}^pE_0$, ${}^pE_1$ etc.) and ${}^pI_i$ (${}^pI_0$, ${}^pI_1$ etc.). ${}^tE_i$ is equal to ${}^pE_i$, but ${}^tI_i$ is not generally equal to ${}^pI_i$, since ${}^pI_i$ contains all contributions from the parent nuclide decay. We refered the typical gamma ray depopulating the isomeric state having the energy ${}^tE_0$ and the intensity ${}^tI_0$. Then, we compare a gamma-ray energy and the level energies connected by the gamma ray in the parent nuclide decay with those in the isomeric state decay. If the corresponding gamma-ray energies and the level energies are equal, the gamma-ray intensity ${}^pI_i'$ having no contibutions of the isomeric state is derived by the next equation,

$${}^pI_i' = {}^pI_i - ({}^pI_0 / {}^tI_0) \cdot {}^tI_i .$$

By these procedure, we produced a decay data library. This library includes the decay data of 1281 nuclides. The decay data in the ENSDF are based on experimental work, thus the data for nuclides not measured by

experiment are lacked in the ENSDF. We made up for these data as will be mentioned in section 4.2. and produced JDDL library.

3. Calculation of Decay Power and Gamma-Ray Spectrum

Decay power and gamma-ray spectra were calculated for the instantaneous burst of fissions by FPGS code[5] which analyzes build-up and decay of fission products. In the case of the instantaneous burst of fission, the cross section or the neutron flux data are not needed and only the nuclear decay and fission yield data are required. The decay data were taken from the ENSDF as mentioned in section 2. For the fission yield, the data of the ENDF/B-IV [6] were used.

In nuclear fission, many fission products of which experimental data (half-life, decay energy etc.) have not been known because of the short half-lives are also produced in non-negligible yields. They decay to the nuclides with longer half-lives following the decay chain in a very short time. In the calculation of decay power, such neutron-rich nuclides far from the stability line should be taken into consideration and their beta and gamma-ray energy releases are estimated by some theoretical model with Q-values derived from mass formula. In the ENDF/B-IV, the yield data are evaluated including such nuclides. In the ENSDF, however, the nuclides without the experimental data are not included. Therefore, the net independent yield for the nuclides with no experimental data are transfered into the cummulative yield of the first appearing nuclide in each decay chain in the ENSDF.

The experimental data are usually expressed in a burst function $f(t)$ (MeV/sec), which is defined as the rate of energy release at t sec after fission burst. For the presentation purpose, it has become common practise to illustrate the pulse function $tf(t)$ (MeV/fission). The burst function $f(t)$ may be estimated from the data of finite irradiation time if the cooling time is measured between the midpoint of the irradiation and the counting interval,

$$T_c = T_w + (T_r + T_{ct}) / 2 ,$$

where T_w, T_r, and T_{ct} are a waiting time from the end of the irradiation to the begining of the counting, an irradiation time and a counting time, respectively. The deviation from the exact value may be small if $T_w \gg T_r + T_{ct}$.

4. Calculated Result

4.1. Calculation with decay data of the ENSDF only

The results of the calculated decay power $tf(t)$ for ^{235}U thermal fission are shown by a dashed line in Figs.3 - 5. The experimental data which were taken from the paper by Dickens et al.[7] are shown by open circles with error bars.

In Figs.6 - 13, the calculated gamma-ray spectra at various cooling times after fission burst are shown. The dashed lines are the calculated spectra and the triangles with error bars are the experimental spectra which are taken from the tabulated data in ref. 8). The original data are given in unit of photons/MeV/fission on a pointwise basis. We converted the data to be in unit of photons·MeV/fission by multipling the photon energy and the energy interval between the successive data points as used by LASL (Los Alamos Scientific Laboratory) group[12] . Because, by using this unit, the integral of the spectrum thus obtained is proportional to the decay power $tf(t)$, and we can examine both gamma decay power and gamma-ray spectrum on a same basis.

As shown in these figures, the calculated decay power and gamma-ray spectra are considerably underestimated at short cooling times after fission burst. Especially for the gamma decay power, the discrepancies are large. At long cooling times, however, the agreements are improved for the decay power and the gamma-ray spectra except for high energy part.

The similar treatment was applied to the estimation of ^{239}Pu thermal fission. The results are shown in Figs.14 - 24. The experimental data were taken from ref.9) and 10). The similar features mentioned above for ^{235}U thermal fission are seen in these figures.

4.2. Calculation with modified decay data library (JDDL)

The calculated decay power and gamma-ray spectra using only the ENSDF data were underestimated by comparing with the experimental data at short cooling times ($< 10^3$ sec). To search the cause of these discrepancies we compared our decay chains and the average energies per decay with the JNDC library[11] which was estimated by Working Group on Evaluation of Decay Heat of Japanese Nuclear Data Committee and was successfully used for decay power calculations.

Examples of the decay chains for mass number 66 - 74 are shown in Figs. 25 - 26. In Fig.25 the decay chain diagrams from the ENSDF and in Fig.26 those of the JNDC library are shown. From these figures, it is found out that the decay chains from the ENSDF are generally shorter than those of the JNDC at neutron-rich side. The decay data in the ENSDF are based on the experimental work. Thus the data for nuclides with short half-lives which are very difficult to be measured by experiment are lacked in the ENSDF. However, the fission products include many neutron-rich nuclides with short half-lives of which data are important for the decay heat calculation because of the non-negligible fission yields. These data are estimated by theoretical model in the JNDC library and the decay chains are extended longer at neutron-rich side. When we added those estimated data in the JNDC libtary to our decay data library, the calculated values for ^{235}U and ^{239}Pu thermal fission are rather improved as shown in Figs.27 - 32. Especially the calculated beta decay power agreed fairly well with the experimantal data within the error bars. The gamma decay power was, however, still underestimated at short cooling times.

In the JNDC library the average energies per decay of 87 nuclides with large Q-values (> 5 MeV) are also replaced by theoretically estimated values, even though the experimental data are exist, since the data for such short-lived nuclides are often not so reliable at the present stage[11] . They

are shown in table 1 taken from ref.11). We also replaced such data and produced JDDL library. In Figs.33 - 38 the calculated results with the JDDL library are shown. The agreements with the experimental data were further improved. However, for the gamma decay power, the calculated results are overestimated for ^{235}U thermal fission at 10^3 to 10^4 sec cooling times and underestimated for ^{239}Pu thermal fission at short cooling times.

5. Discussion

In Figs.39 - 44, the comparison of estimated values of decay power between the JDDL library, the JNDC library and the ENDF/B-IV for ^{235}U and ^{239}Pu thermal fission and their C/E values (the calculated value devided by the experimental one) are shown. For the beta decay power of ^{235}U and ^{239}Pu , the present results are slightely larger than those with the JNDC library. But the C/E values are within ± 10 % of 1.0 and these results are expected to be acceptable. The results with the ENDF/B-IV are very different from the experimental data for beta and total decay power. For the gamma decay power, in the case of ^{235}U thermal fission, the present results are smaller than those with the JNDC library. However, at long cooling times ($> 10^2$ sec), the present results are more close to the experimental results. The data in the JNDC at these cooling times are considered to be overestimated. In the case of ^{239}Pu thermal fission, the present results are underestimated at short cooling times. This feature is also seen for ^{235}U thermal fission. The data of the nuclides with short half-lives in the JDDL library may not be satisfied yet.

In the JDDL library, the fission yield data of the ENDF/B-IV are used, but in the JNDC library, the most of the independent fission yield data are taken from the compilation by Rider and Meek[13] and newly calculated data are also included. The study on the influence of such different yield data on the decay power may be needed to understand the discrepancy.

For the gamma-ray spectra, we could not compare with the other library. Because there are no spectral data in the JNDC library and the ENDF/B-IV. At short cooling times, there is a problem how to estimate the spectra for nuclides with no experimental informations. In the present work, only the nuclides with experimental data are taken into account. Thus, at short cooling times, the calculated spectra are underestimated. Then for the calculation of the gamma-ray spectra it may be needed to estimate the

gamma-ray spectral data of nuclides with short half-lives by theoretical model. If the spectral data may be obtained by theoretical model, further understanding for the decay power will be acquired.

In conclusion, the decay data from the ENSDF at present status are not directly applicable to the calculation of decay power and gamma-ray spectra at short cooling times ($< 10^3$ sec), because the calculated results are inevitably underestimated. One reason is lack of the necessary experimental data in the ENSDF, which are important because of their non-negligible yields, but are very difficult to measure due to their very short half-lives. It leads to insufficient decay chains for the present purpose. Another one is existance of a lot of nuclides with insufficient experimental data, especially those with high Q-values. In this case, the average energies per decay should be estimated by theoretical model as mentioned in ref.11). Compensating the ENSDF with the theoretical values, the experimental data are reproduced by the calculation except for the spectra at short cooling times. At long cooling times ($> 10^3$ sec), the decay data of the ENSDF at present status are sufficiently applicable.

The partly revised ENSDF would be obtained twice a year. As progressing the evaluating work, the data file will become much applicable. However, it is very difficult to measure the decay data of nuclides with short half-lives by experiment. Then the direct application of the ENSDF to the calculation of decay power and gamma-ray spectra may be limited. Thus some kinds of estimation may be needed on the decay data of nuclides with short half-lives.

Acknowledgements

The authors wish to express their thanks to Mr. H. Ihara for his help to preparing calculation codes, and to Dr. T. Tamura and Dr. Z. Matumoto from whom the authors were offered the ENSDF data file. In particular, the helpful discussion with Dr. Z. Matumoto is appreciated.

They are also grateful to Dr. M. Hirata and Dr. K. Sato for their interest on this work.

References

1) Lederer C.M. et al.: "Table of Isotopes, 7th edition," John Wiley & Sons, Inc., (1978).

2) Ewbank W.B. (Ed.): "Nucler Data Sheets," Academic Press, (1966 -).

3) Ewbank W.B. et al.: "Evaluated Nuclear Structure Data File, A manual for preparation of data sets," ORNL-5054/RI (1978).

4) Martin M.J. (Ed.): "Nuclear Decay Data for Selected Radionuclides," ORNL-5114 (1976).

5) Ihara H. et al.: "Revised FPGS-3 Program and Revision of Nuclear Data and γ-Ray Library," private communication (in Japanese) (1982)

6) ENDF/B Summary Document BNL-NCS-17541 2nd edition (1975).

7) Dickens J.K. et al.: "Fission-Product Energy Release for Times Following Thermal-Neutron Fission of ^{235}U Between 2 and 14000 seconds," ORNL/NUREG-14 (1977).

8) Dickens J.K. et al.: "Delayed Beta- and Gamma-Ray Production Due to Thermal-Neutron Fission of ^{235}U, Spectral Distributions for Times After Fission Between 2 and 14000 sec : Tabular and Graphical Data," ORNL/NUREG-39 (1978).

9) Dickens J.K. et al.: "Fission-Product Energy Release for Times Following Thermal-Neutron Fission of ^{239}Pu Between 2 and 14000 seconds," ORNL/NUREG-34 (1978).

10) Dickens J.K. et al.: "Delayed Beta- and Gamma-Ray Production Due to Thermal-Neutron Fission of ^{239}Pu : Tabular and Graphical Spectral Distributions for Times After Fission Between 2 and 14000 sec," ORNL/NUREG-66 (1980).

11) Yamamoto T. et al.: "JNDC FP Decay Data File," JAERI-M 9357 (1981).
Ihara H. et al.: "JNDC FP Decay and Yield Data," JAERI-M 9715 (1981).
Yoshida T. and Nakasima R.: J. Nucl. Sci. Tech. 18 (1981) 393.

12) England T.R. and Stamatelatos M.G.: "Comparisons of Calculated and

Experimental Delayed Fission-Product Beta and Gamma Spectra from ^{235}U Thermal Fission," LA-NUREG-6896-MS (1977).

13) Rider B.F. and Meek M.E.: "Compilation of Fission Product Yield," NEDO-12154-2(D) (1977).

Table 1 Comparison with Experimental and Estimated Values of Average Decay Energies for Nuclides with Q_β > 5 MeV

NO.	NUCL.	HALF LIFE (SEC)	Q-BETA (MEV)	EXPERIMENT E-TOTAL (MEV)	EXPERIMENT E-BETA (MEV)	EXPERIMENT E-GAMMA (MEV)	ESTIMATE E-TOTAL (MEV)	ESTIMATE E-BETA (MEV)	ESTIMATE E-GAMMA (MEV)
1	CU 68M	2.250000D+02	5.3410	1.1673	0.1883	0.9791	1.1530	0.1970	0.9560
2	CU 70M	4.600000D+01	6.3100	4.5071	1.5758	2.9312	3.8170	1.6500	2.1670
3	CU 70	4.500000D+00	6.1700	3.1447	2.9688	0.5759	2.9920	2.6970	0.2950
4	GA 74	4.950000D+02	5.4000	4.0724	1.0245	3.0479	3.6890	1.2880	2.4010
5	GA 76	2.710000D+01	6.7700	4.9975	1.8051	2.7925	4.2420	1.7460	2.4960
6	AS 80	1.650000D+01	5.7000	2.9287	2.3200	0.6086	2.7380	2.4790	0.2590
7	GE 81	1.010000D+01	5.6000	2.6061	2.4908	0.1153	3.0070	2.1260	0.8810
8	AS 82M	1.300000D+01	7.4000	5.0172	1.8568	3.1604	4.7170	1.9540	2.7630
9	AS 82	2.100000D+01	7.4000	3.7299	3.2534	0.4765	4.9440	1.9900	2.9540
10	AS 83	1.410000D+01	5.4600	4.0071	1.2556	2.7514	2.9930	2.0000	0.9930
11	AS 84	5.800000D+00	9.5540	5.5649	3.9893	1.5756	6.2390	2.8340	3.4050
12	SE 85	3.280000D+01	6.1000	3.9427	1.7038	2.2390	4.0180	1.6300	2.3880
13	SE 86	1.670000D+01	5.1000	3.4952	1.1468	2.3485	3.3140	1.3500	1.9640
14	BR 86	5.570000D+01	7.3000	5.3771	1.7377	3.6395	4.8830	1.9470	2.9360
15	SE 87	5.600000D+00	7.2700	4.4520	2.4920	1.9600	4.7230	2.0790	2.6440
16	BR 87	5.560000D+01	6.5000	5.3982	1.9429	3.8553	4.2230	1.8130	2.4100
17	SE 88	1.530000D+00	7.0000	4.1005	2.3809	1.7195	4.1200	2.4040	1.7160
18	BR 88	1.630000D+01	8.6000	5.0748	2.0177	3.0572	5.6640	2.4540	3.2100
19	RB 88	1.066000D+03	5.3090	2.7275	2.0911	0.6364	3.6870	1.1930	2.4940
20	BR 90	1.920000D+00	10.3300	5.5218	4.3885	1.1333	6.7510	3.0890	3.6620
21	RB 90M	2.580000D+02	6.4670	4.6392	1.2888	3.3503	4.2100	1.5440	2.6660
22	RB 90	1.530000D+02	6.3600	4.0516	1.8875	2.1641	4.3300	1.5710	2.7590
23	KR 91	8.570000D+00	6.2000	3.7231	1.9900	1.7331	3.6720	2.0550	1.6170
24	RB 91	5.820000D+01	5.7000	3.7347	1.5157	2.2190	3.7720	1.4760	2.2960
25	KR 92	1.850000D+00	6.0800	3.1253	2.4086	0.7168	3.3400	2.2620	1.0780
26	RB 92	4.500000D+00	7.7700	3.7554	3.4895	0.2659	4.4220	2.8560	1.5660
27	KR 93	1.289000D+00	8.7000	5.1672	2.8899	2.2772	5.4840	2.7270	2.7570
28	RB 93	5.820000D+00	7.4500	4.1101	2.7167	1.3934	4.8220	2.1470	2.6750
29	SR 95	2.440000D+01	6.0900	3.2969	2.2653	1.0317	4.0350	1.5930	2.4420
30	SR 96	1.015000D+00	5.3600	2.8877	1.9758	0.9119	2.9210	1.9620	0.9590
31	SR 97	4.410000D-01	7.2000	4.0271	2.5420	1.4850	4.1040	2.6030	1.5010
32	Y 97M	1.130000D+00	7.3980	4.2122	2.4020	1.8102	4.1550	2.6830	1.4720
33	Y 97	3.700000D+00	6.6700	3.9652	2.1515	1.8137	3.7030	2.4720	1.2310
34	RB 98	1.080000D-01	10.8500	5.0680	3.8139	1.2542	6.0340	3.7110	2.9230
35	SR 98	6.600000D-01	5.8100	2.7046	2.5348	0.1698	3.1900	2.1390	1.0510
36	Y 98M	2.000000D+00	9.0800	5.7837	2.6783	3.1054	5.5850	2.9890	2.5960
37	Y 98	6.500000D-01	8.9800	4.7593	3.9453	0.8140	5.2570	3.2160	2.0410
38	Y 99	1.400000D+00	6.3900	2.9760	2.4823	0.4936	3.5220	2.3750	1.1470
39	ZR101	2.400000D+00	5.9000	2.8496	2.4966	0.3530	3.2510	2.1600	1.0910
40	TC104	1.092000D+03	5.6200	3.5180	1.0758	1.8422	3.9220	1.2440	2.6780
41	MO105	3.670000D+01	5.4000	2.4100	2.2554	0.1546	3.6550	1.2900	2.3650
42	TC108	5.000000D+00	8.0000	4.0942	3.2938	0.8004	5.2420	2.2490	2.9930
43	RH110M	2.850000D+01	5.4000	3.3658	1.3534	2.2125	3.0140	2.2370	0.7770
44	RH110	3.000000D+00	5.4000	2.4399	2.3839	0.0561	2.6880	2.2020	0.4860
45	AG116M	1.040000D+01	6.3120	3.6176	1.4355	1.6821	3.3560	2.3130	1.0430
46	AG116	1.608000D+02	6.1000	3.5901	2.7232	0.8668	4.2220	1.3970	2.8250
47	AG118M	2.000000D+00	7.1280	1.9551	0.7924	1.1627	1.3410	0.7890	0.5520
48	AG118	3.760000D+00	7.0000	3.8657	2.5388	1.3269	3.9490	2.5150	1.4340
49	AG122	4.800000D-01	9.1700	4.8156	3.6970	1.1185	5.5590	3.0480	2.5110
50	IN122M	1.000000D+01	6.5900	3.6522	1.9173	1.7349	3.9220	2.4230	1.4990
51	IN122	1.500000D+00	6.5100	3.9955	2.7374	1.2582	3.6050	2.3630	1.2420
52	IN124M	2.400000D+00	7.3300	4.5064	2.2336	2.2728	4.2190	2.5580	1.6610
53	IN124	3.210000D+00	7.1400	4.1991	2.3328	1.8662	4.0800	2.5100	1.5700
54	IN125M	1.220000D+01	5.6600	2.5852	2.4518	0.1334	3.4960	1.6600	1.8360
55	IN125	2.320000D+00	5.4800	3.1008	1.8074	1.2934	3.0170	1.9370	1.0800
56	IN126M	2.100000D+00	8.2100	4.1259	3.4662	0.6597	4.8710	2.7740	2.0970
57	IN126	1.530000D+00	8.0800	4.9940	2.4682	2.5257	4.7610	2.7350	2.0260
58	IN127M	3.760000D+00	6.6500	3.2214	2.7947	0.4267	3.9180	2.1910	1.7270
59	IN127	1.300000D+00	6.4900	3.0940	2.1763	1.5177	3.6950	2.2520	1.4430
60	IN128M	5.600000D+00	9.3900	6.4546	2.4914	3.9631	6.1910	2.6340	3.5570
61	IN128	8.400000D-01	9.3100	6.3181	3.3628	3.1553	5.8820	3.0490	2.8330
62	IN129M	2.500000D+00	7.8000	3.4898	3.2930	0.1968	5.1020	2.1550	2.9470
63	IN129	9.900000D-01	7.6000	4.2678	2.4574	1.8104	4.4490	2.5880	1.8610
64	IN130	5.760000D-01	9.4000	5.3684	3.1277	2.2406	5.7560	3.0630	2.6930
65	IN131	2.700000D-01	8.0000	4.2296	2.2892	1.9404	4.7240	2.7070	2.0170
66	SN131M	6.100000D+01	5.0500	2.8014	1.1688	1.6326	3.4890	1.0980	2.3910
67	IN132	1.300000D-01	9.8000	7.0172	2.2392	4.7779	6.0540	3.1580	2.8980
68	SB132	1.680000D+02	5.6000	3.7719	1.1976	2.5743	3.9250	1.1970	2.7280
69	SN133	1.470000D+00	7.2400	3.4845	3.0993	0.3852	4.2710	2.4100	1.8610
70	SB134M	1.040000D+01	8.4000	5.1622	3.1359	2.0262	5.5560	2.2840	3.2720
71	SB134	8.500000D-01	8.4000	3.8441	3.8441	0.0000	5.0370	2.7810	2.2560
72	TE135	1.920000D+01	6.2000	3.1299	2.4439	0.6859	4.1520	1.5320	2.6200
73	I 136M	4.480000D+01	7.0000	4.3073	2.3052	2.0021	4.7020	1.7600	2.9420
74	I 136	8.510000D+01	7.0000	4.5202	2.0562	2.4660	4.7020	1.7600	2.9420
75	I 137	2.450000D+01	5.5000	2.7211	1.9721	0.7490	3.7320	1.2720	2.4600
76	CS138M	1.740000D+02	5.4200	0.9285	0.4014	0.5272	1.0140	0.2800	0.7340
77	CS138	1.932000D+03	5.3400	3.3789	1.2474	2.3314	3.7690	1.0890	2.6800
78	XE139	3.950000D+01	5.0200	2.8201	1.7350	0.8851	3.2410	1.0020	2.2390
79	CS140	6.370000D+01	6.1700	3.9679	1.7518	2.2161	4.2200	1.4290	2.7910
80	XE141	1.730000D+00	6.1500	3.4004	2.3649	1.0355	3.5370	2.0480	1.4890
81	CS141	2.490000D+01	5.1900	2.7557	2.0887	0.6669	3.4110	1.2760	2.1350
82	XE142	1.240000D+00	5.0400	3.0388	1.8468	1.1920	2.7350	1.7580	0.9770
83	CS142	1.710000D+00	7.2800	6.4356	2.6237	3.8119	4.2360	2.4490	1.7870
84	LA144	4.210000D+01	5.5000	3.1013	1.7875	1.3138	3.4290	1.3380	2.0910
85	LA146	8.500000D+00	6.3000	3.1771	2.4593	0.7178	3.5270	2.1820	1.3450
86	LA148	1.290000D+00	6.3000	3.0185	2.7429	0.8756	3.5360	2.1750	1.3610
87	PR150	6.200000D+00	5.7000	2.5743	2.3121	0.2622	3.0930	2.0170	1.0760

footnote ; This table is refered from ref. 11).

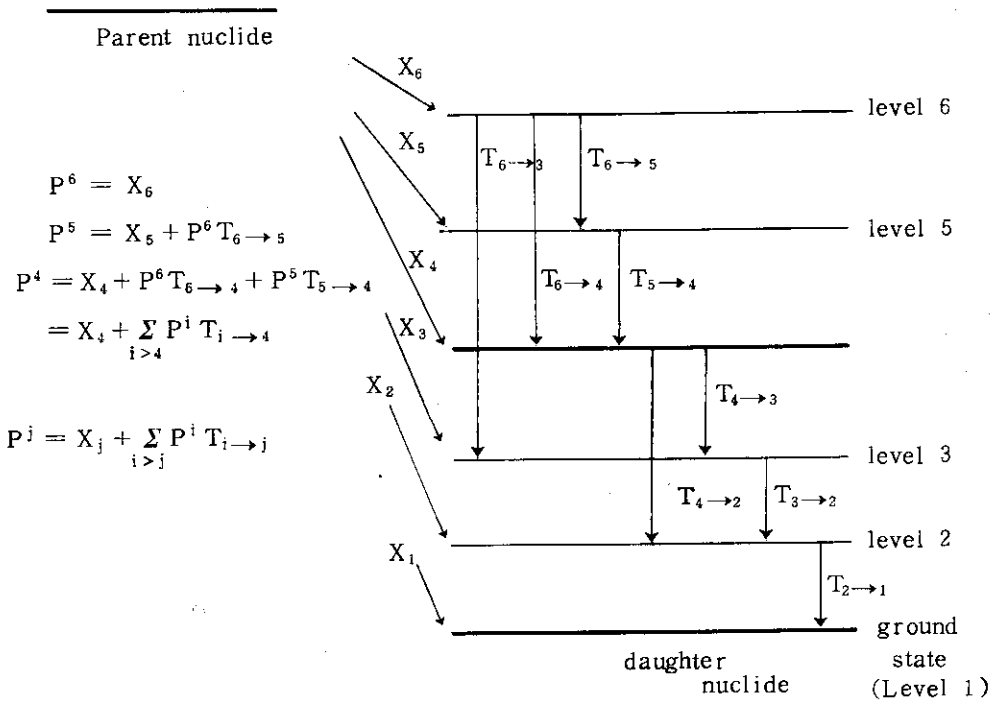

Fig.1 Schematic explanation for the calculation of the branching ratio. The daughter nuclide has the isomeric state. The branching ratio to the isomeric state is calculated from the decay scheme.

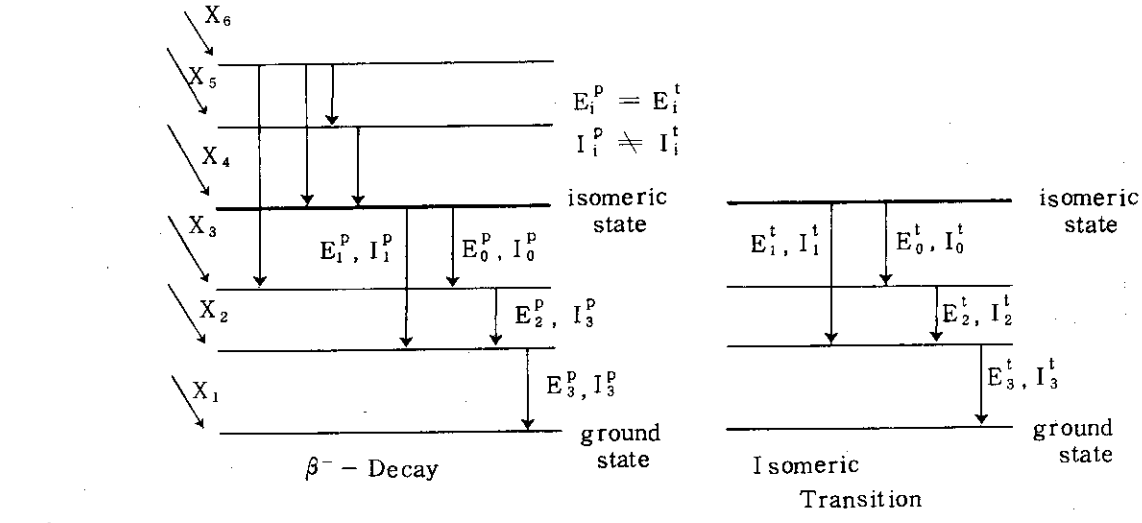

Fig.2 Schematic explanation for the gamma-ray intensity. If the daughter nuclide has the isomeric state, the gamma-ray intensity of the daughter nuclide is derived by eliminating the intensity of the gamma ray through the isomeric state.

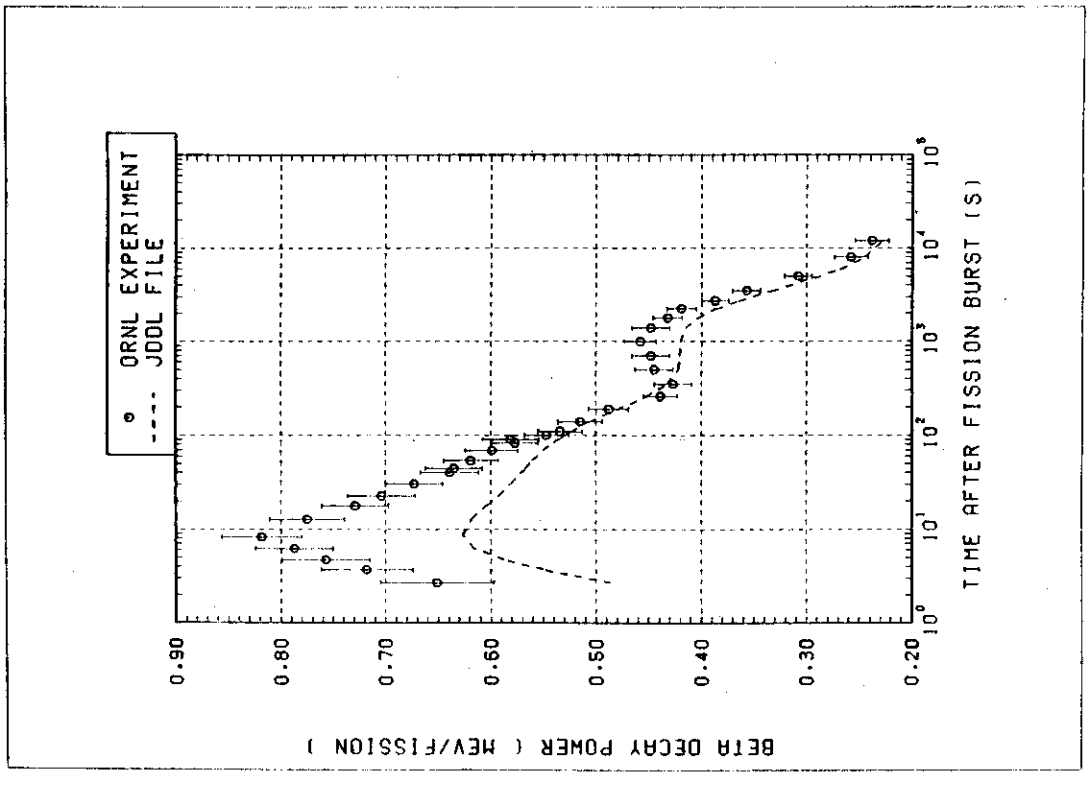

Fig.3 Beta decay power for ^{235}U thermal fission. The dashed line is a calculated decay power with the decay data library produced from only the ENSDF data. The open circles with the error bars are the experimental results by ORNL.

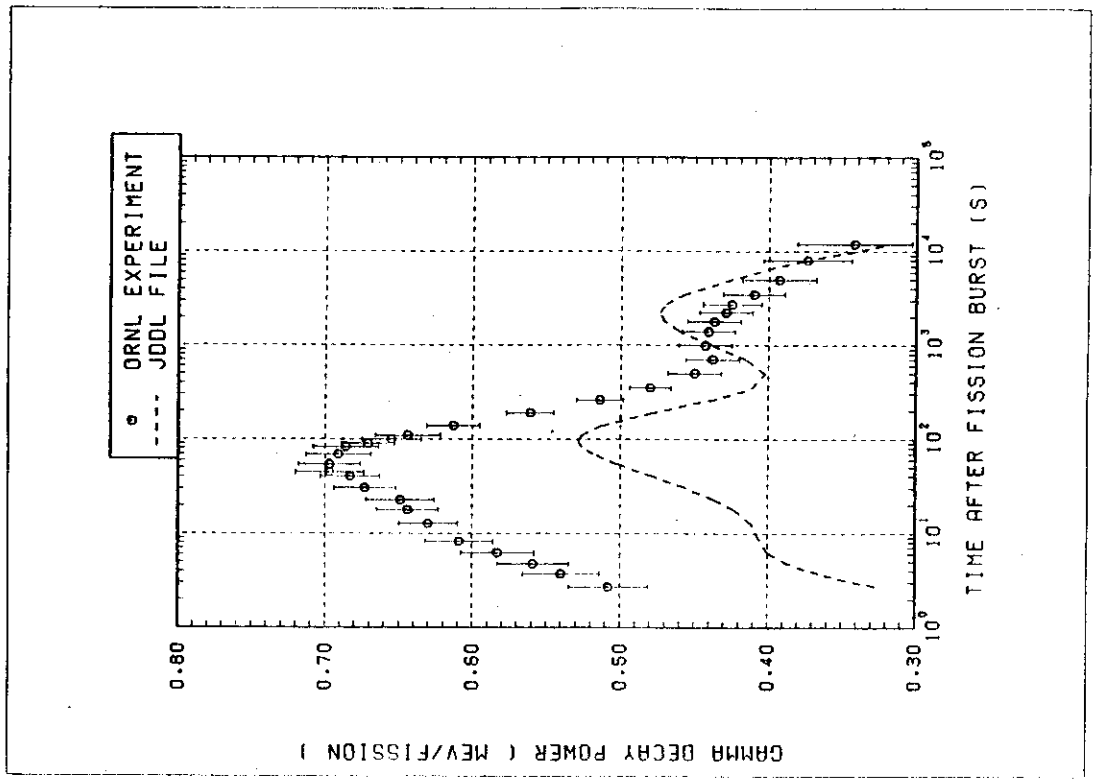

Fig.4 Gamma decay power for ^{235}U thermal fission. The notations are the same as in Fig.3.

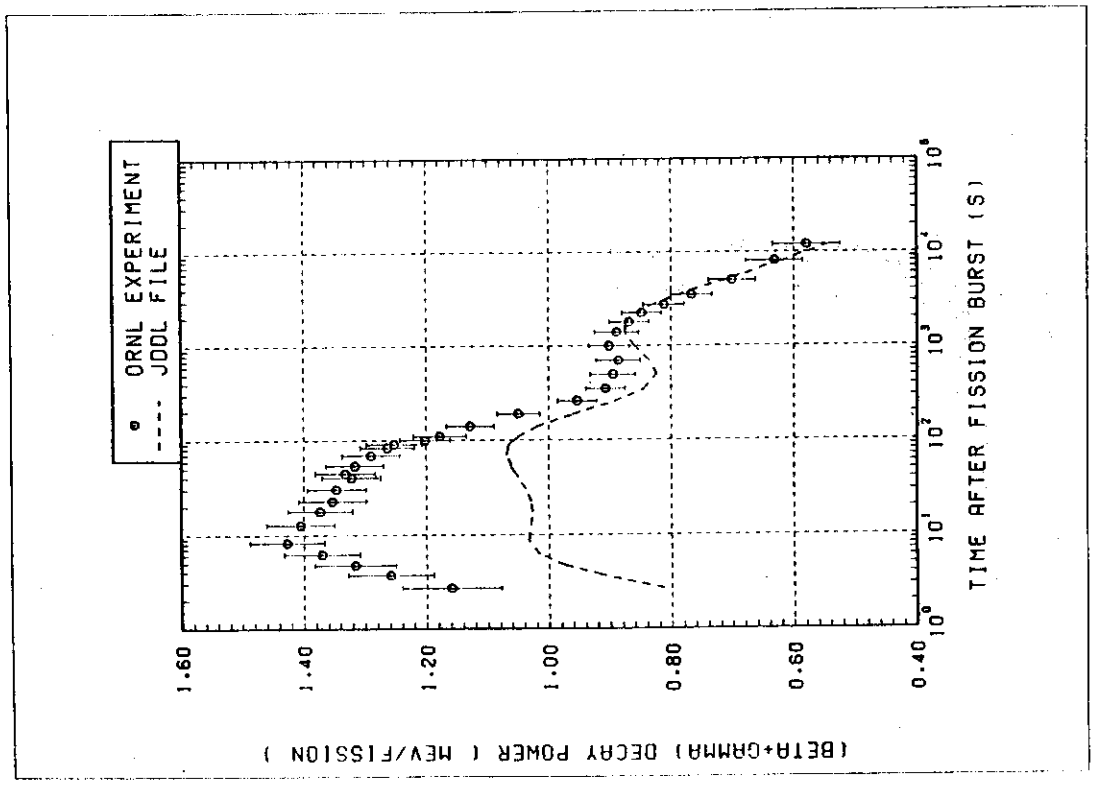

Fig.5 Total decay power for ^{235}U thermal fission. The notations are the same as in Fig.3.

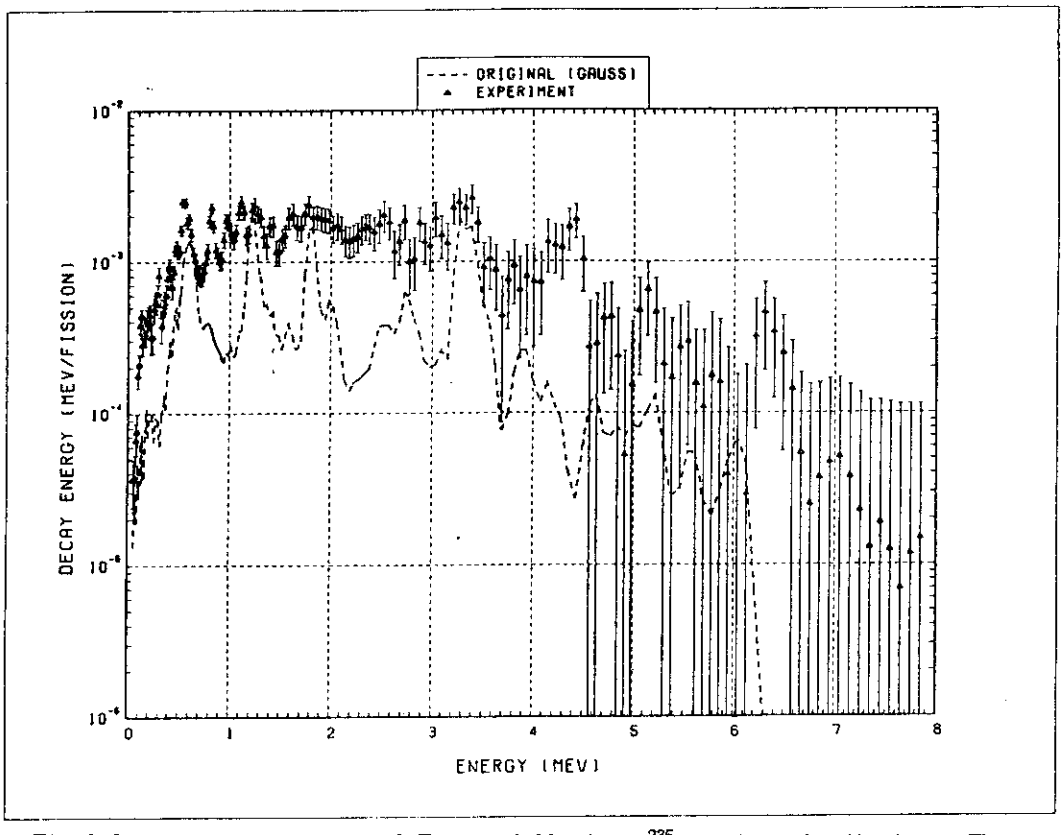

Fig.6 Gamma-ray spectrum at 2.7 sec following ^{235}U thermal fission. The dashed line is a calculated spectrum with decay data library from only the ENSDF data. The triangles with error bars are the experimental results by ORNL.

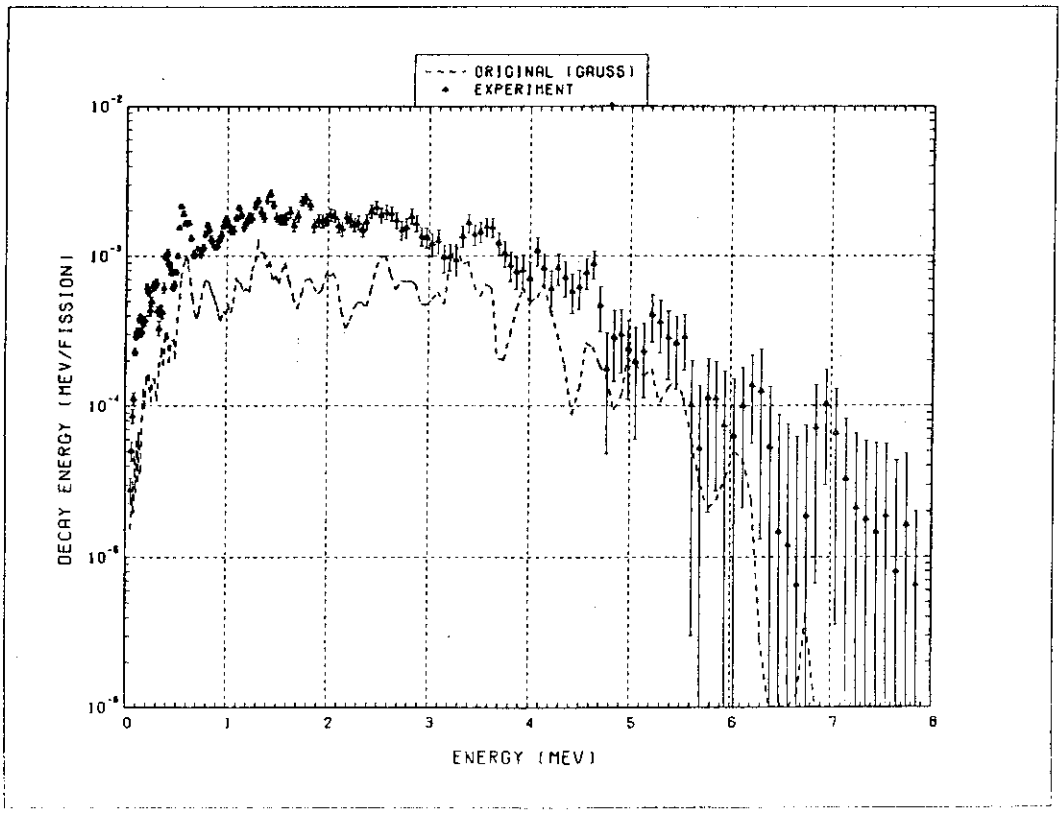

Fig.7 Gamma-ray spectrum at 17.7 sec following ^{235}U thermal fission. The notations are the same as in Fig.6.

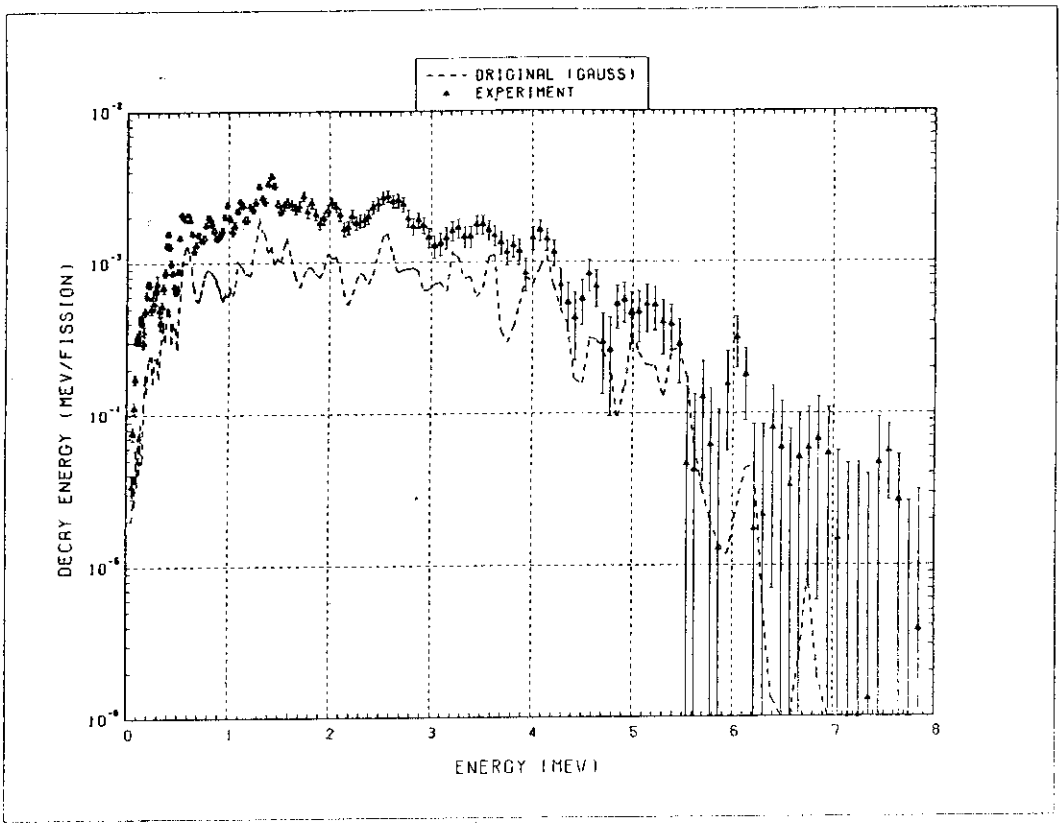

Fig.8 Gamma-ray spectrum at 30.2 sec following ^{235}U thermal fission. The notations are the same as in Fig.6.

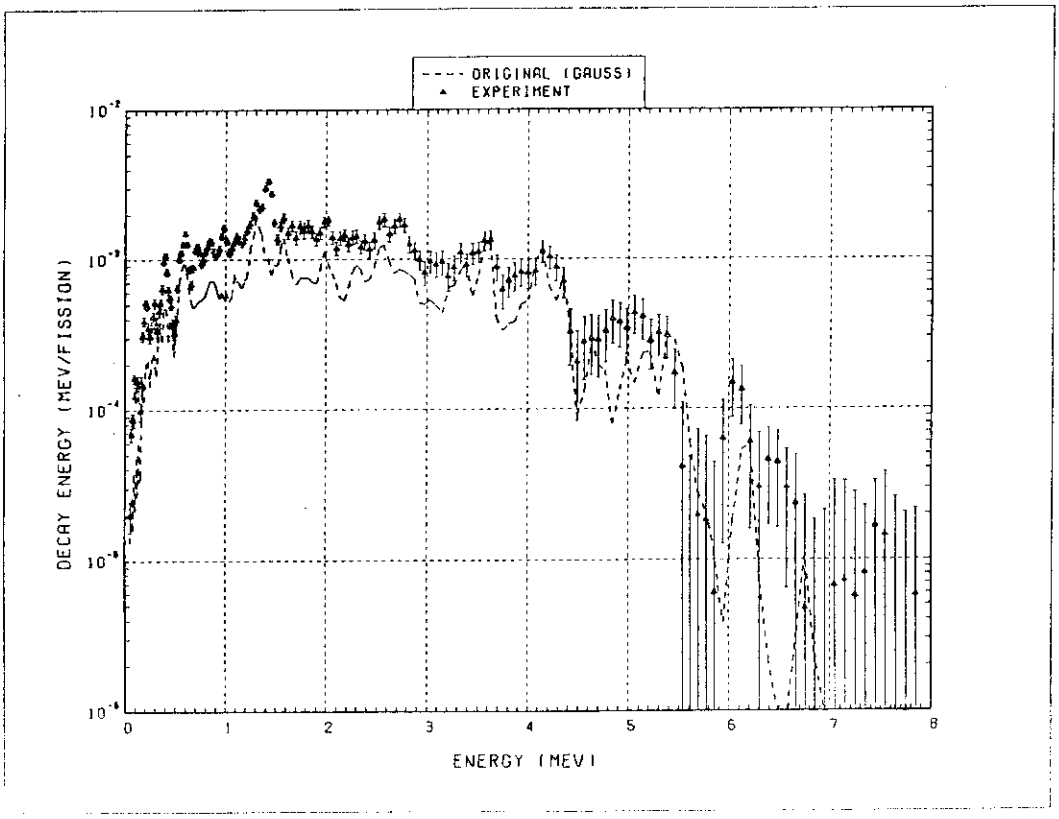

Fig.9 Gamma-ray spectrum at 90.0 sec following ^{235}U thermal fission. The notations are the same as in Fig.6.

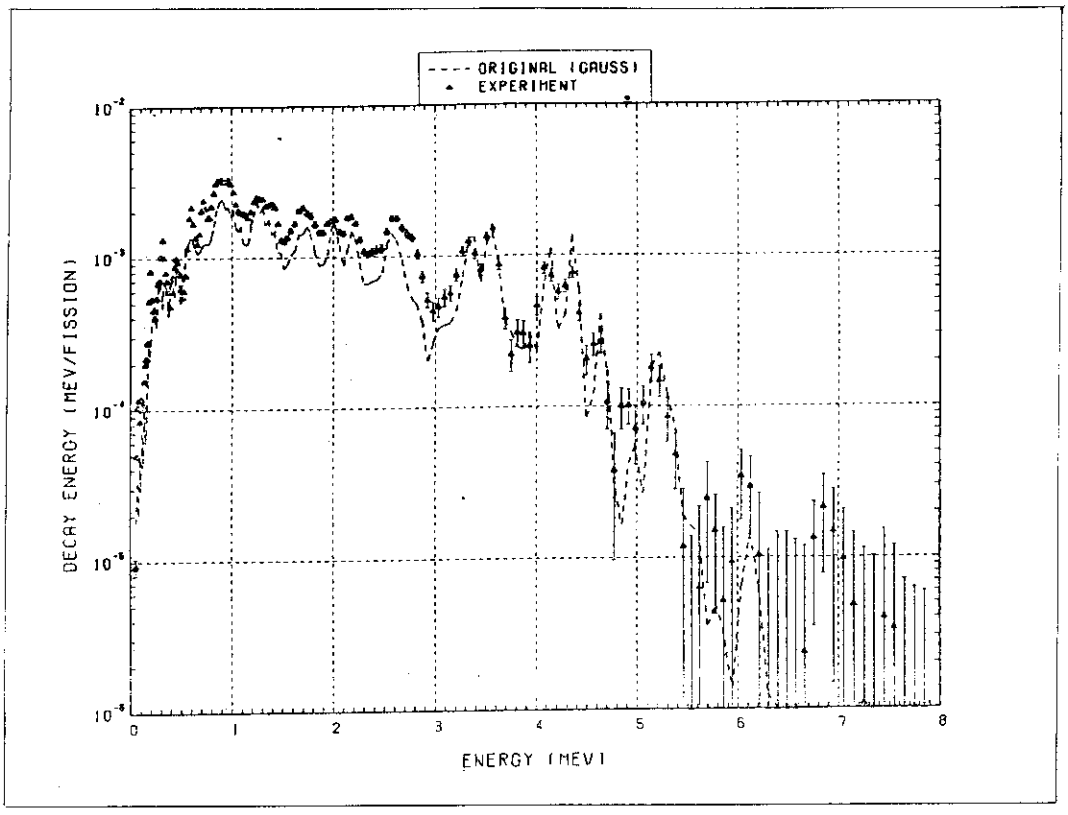

Fig.10 Gamma-ray spectrum at 500.0 sec following ^{235}U thermal fission. The notations are the same as in Fig.6.

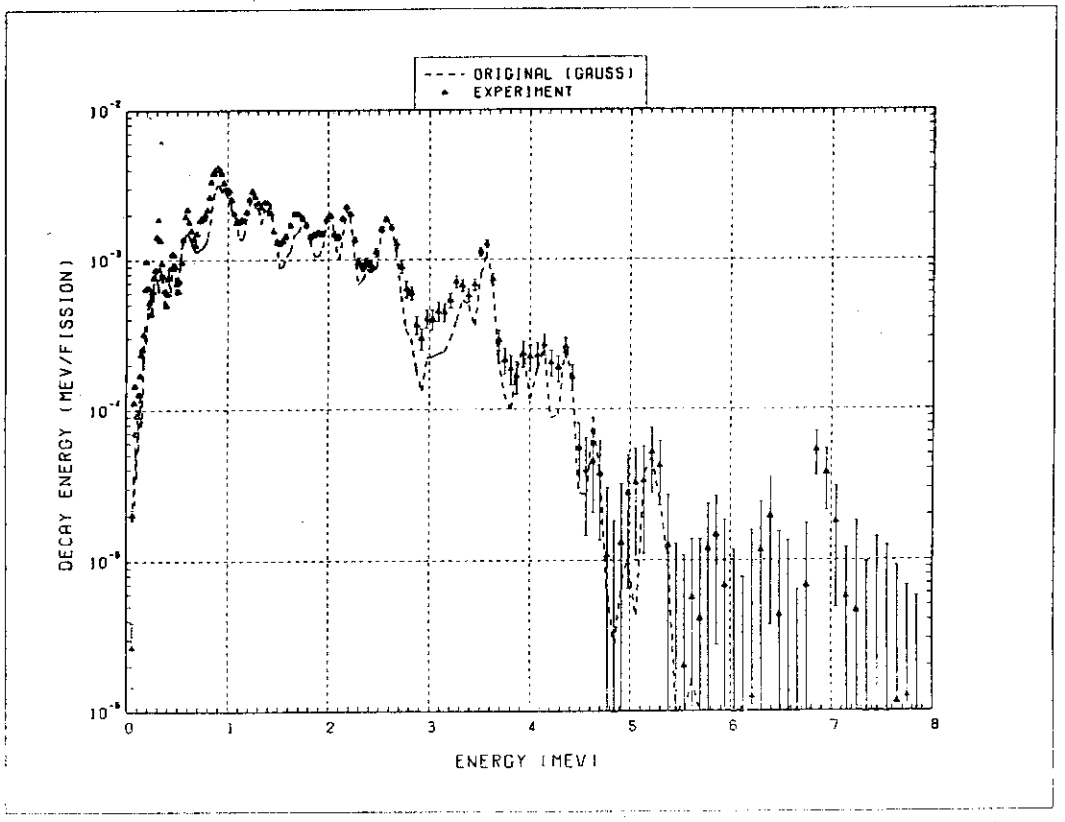

Fig.11 Gamma-ray spectrum at 1000.0 sec following ^{235}U thermal fission. The notations are the same as in Fig.6.

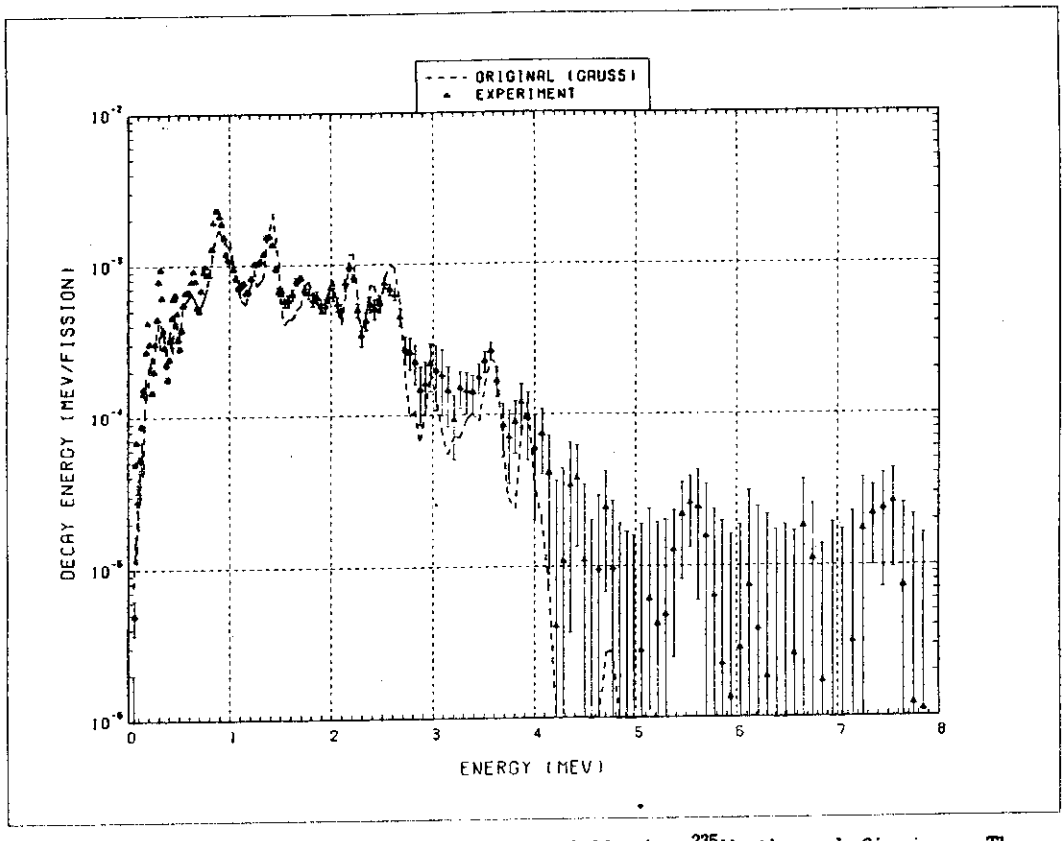

Fig.12 Gamma-ray spectrum at 2750.0 sec following ^{235}U thermal fission. The notations are the same as in Fig.6.

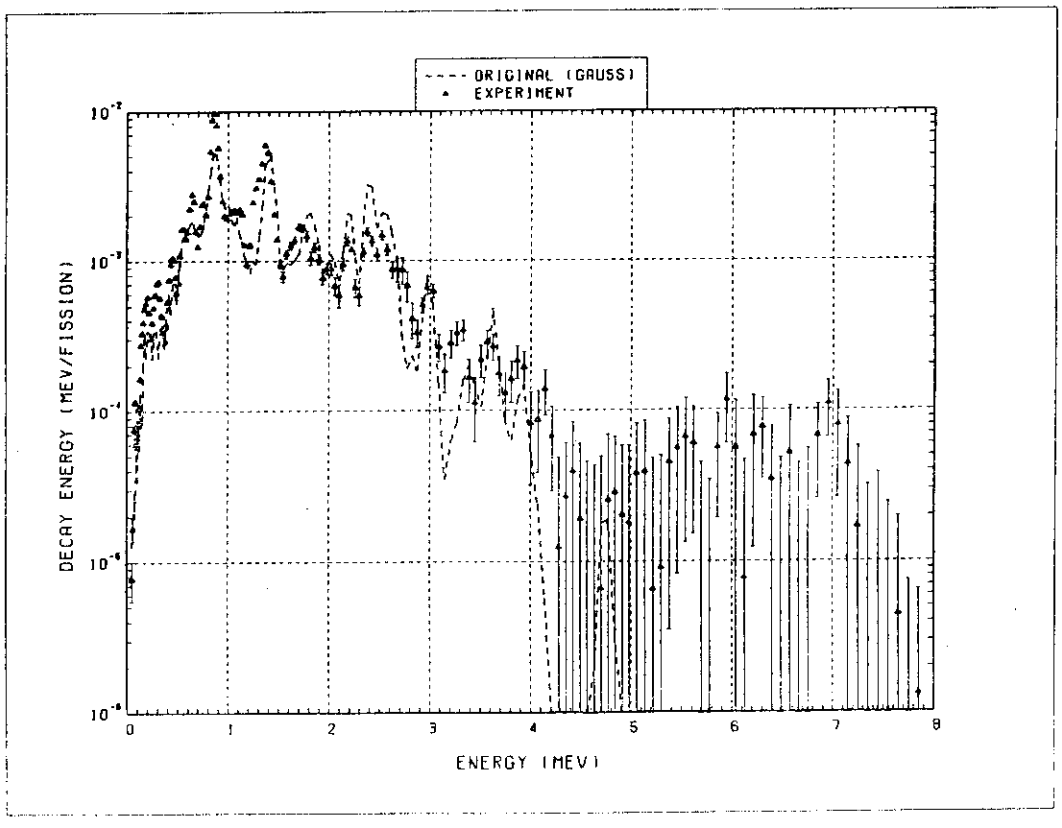

Fig.13 Gamma-ray spectrum at 8000.0 sec following ^{235}U thermal fission. The notations are the same as in Fig.6.

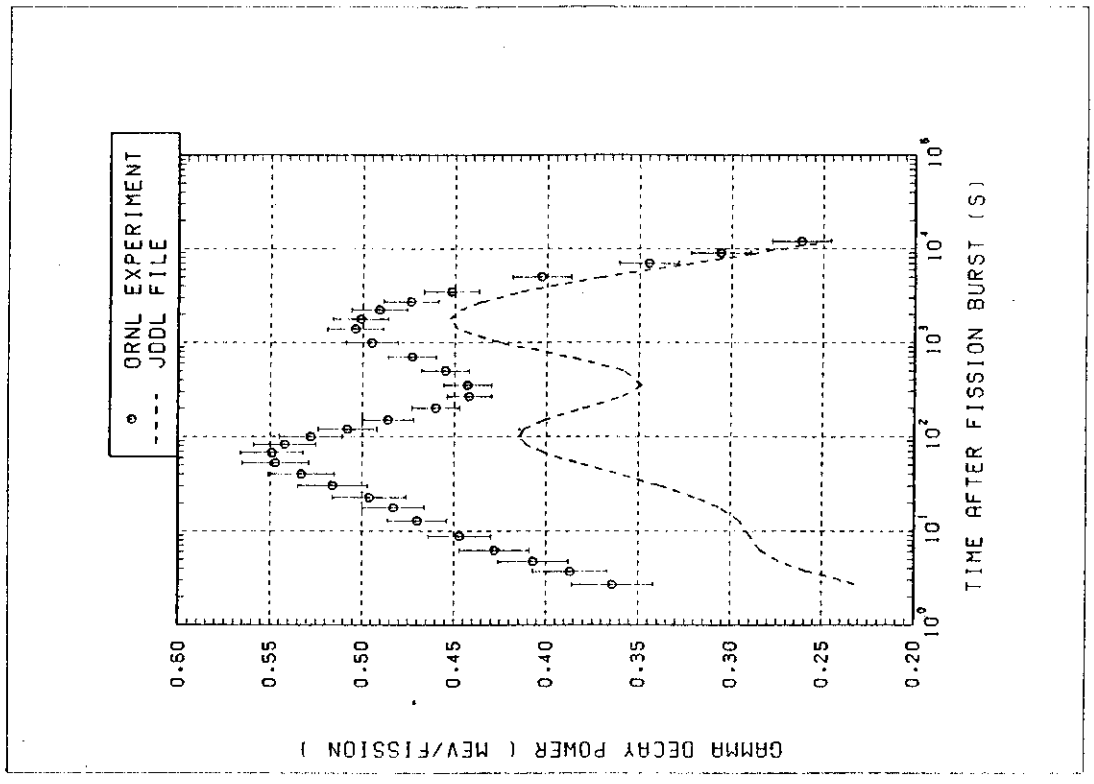

Fig.15 Gamma decay power for ^{239}Pu thermal fission. The notations are the same as in Fig.3.

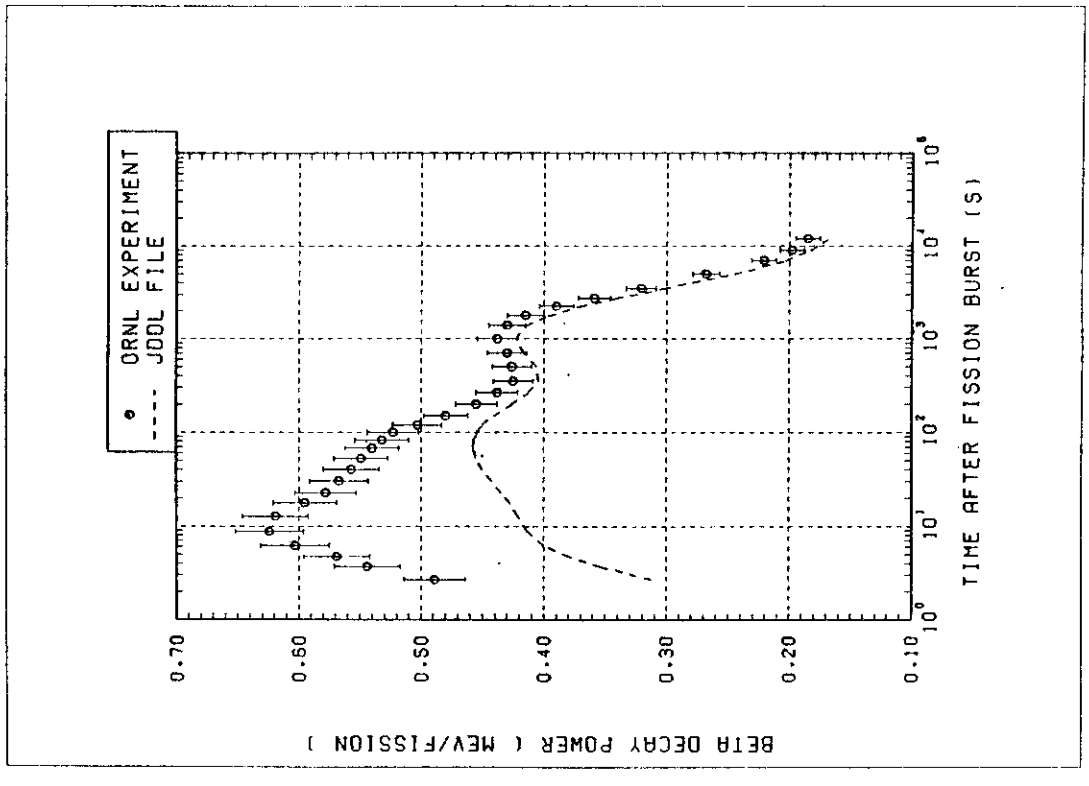

Fig.14 Beta decay power for ^{239}Pu thermal fission. The notations are the same as in Fig.3.

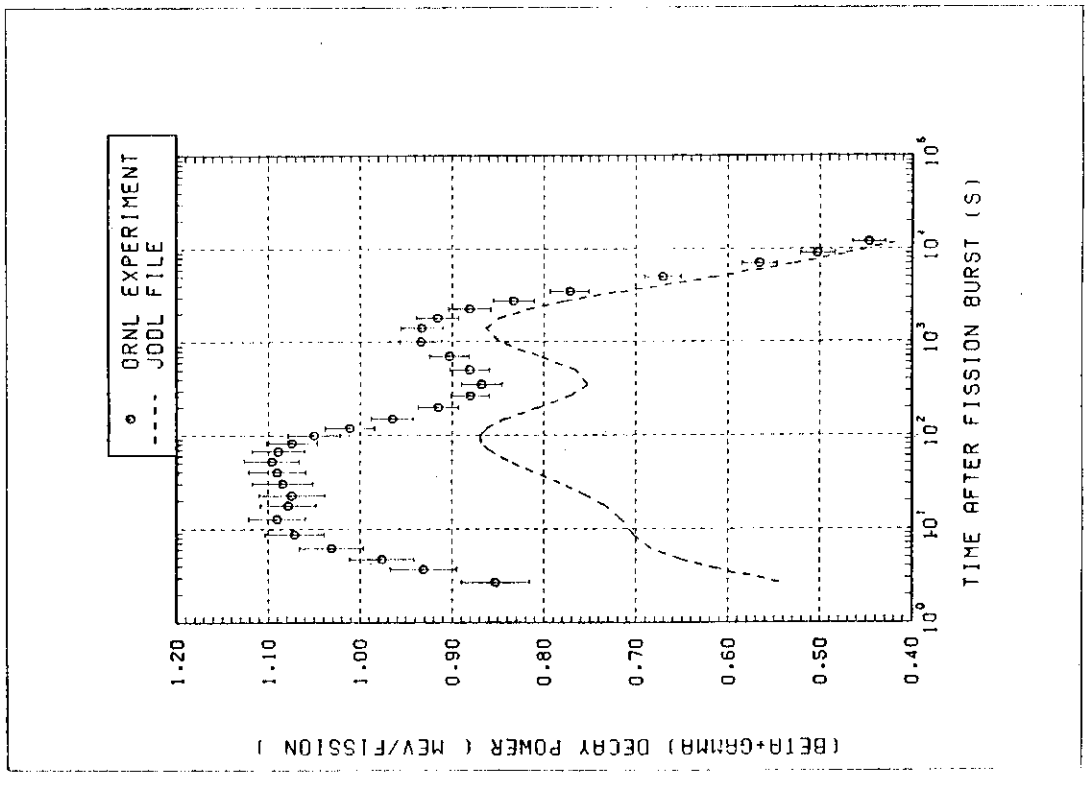

Fig.16 Total decay power for ^{239}Pu thermal fission. The notations are the same as in Fig.3.

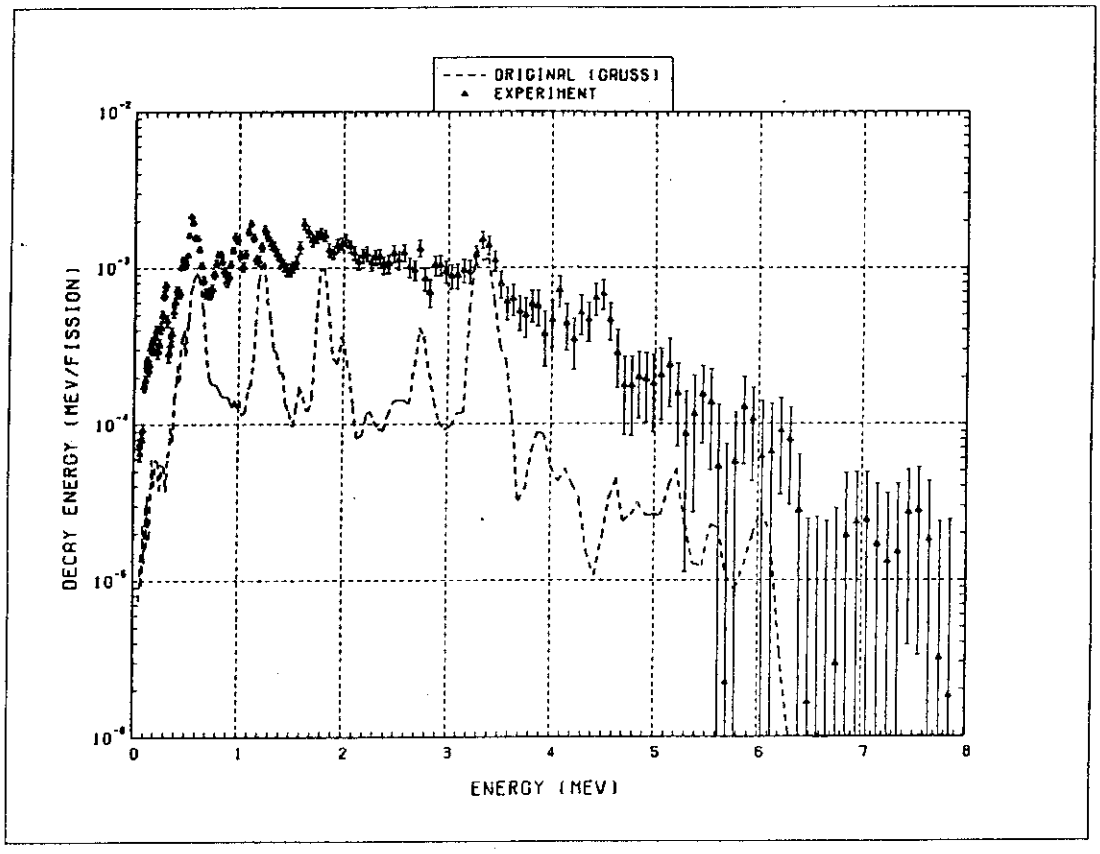

Fig.17 Gamma-ray spectrum at 2.7 sec following ^{239}Pu thermal fission. The notations are the same as in Fig.6.

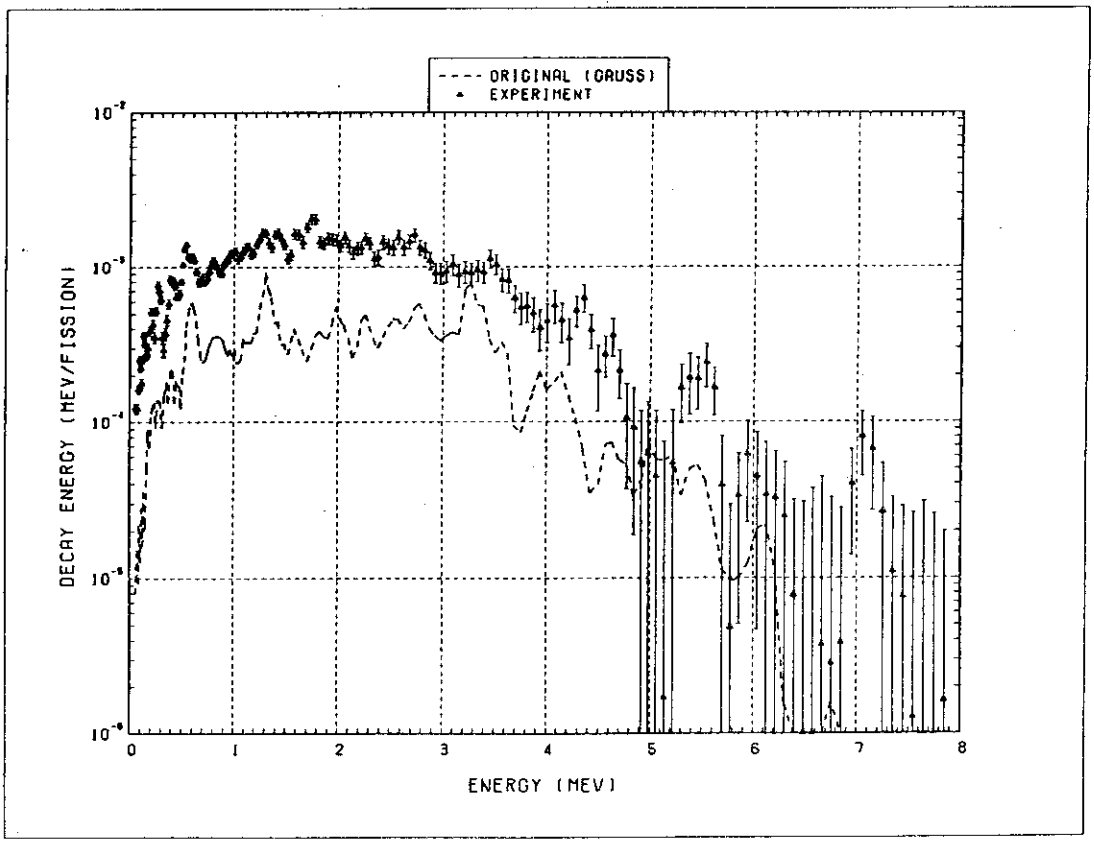

Fig.18 Gamma-ray spectrum at 17.7 sec following ^{239}Pu thermal fission. The notations are the same as in Fig.6.

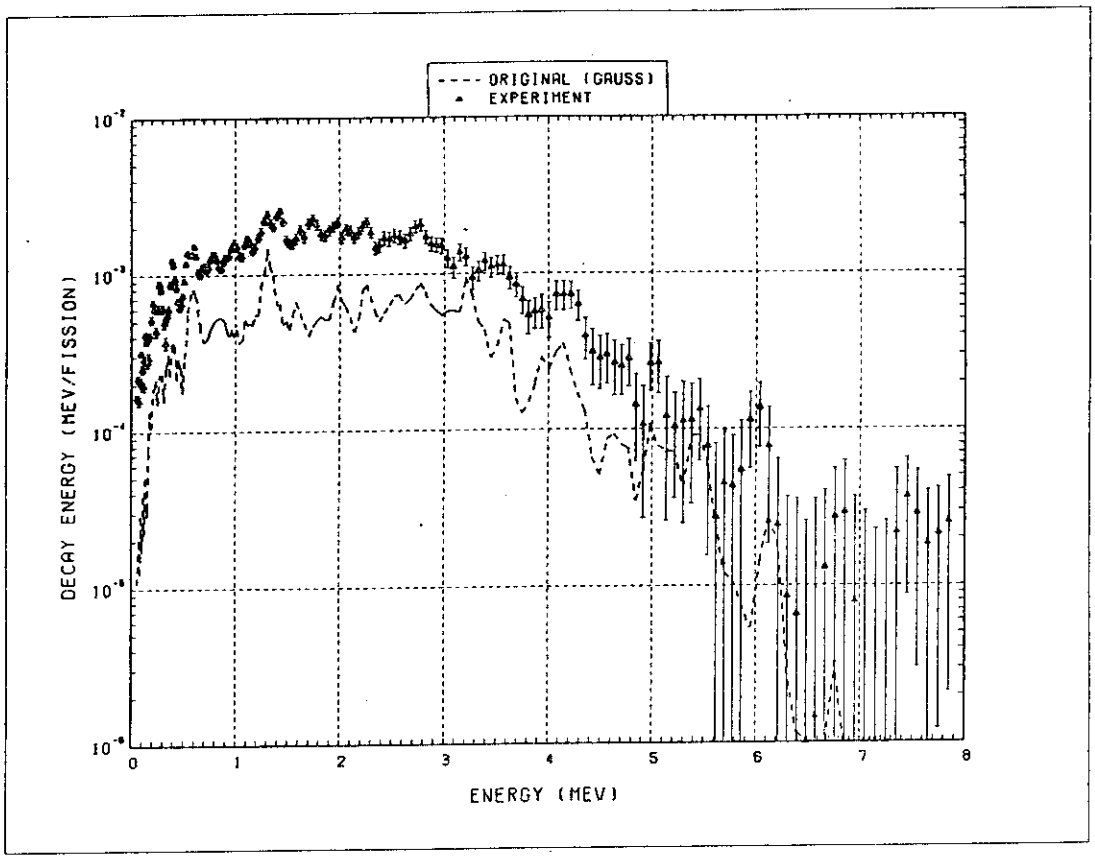

Fig.19 Gamma-ray spectrum at 30.2 sec following ^{239}Pu thermal fission. The notations are the same as in Fig.6.

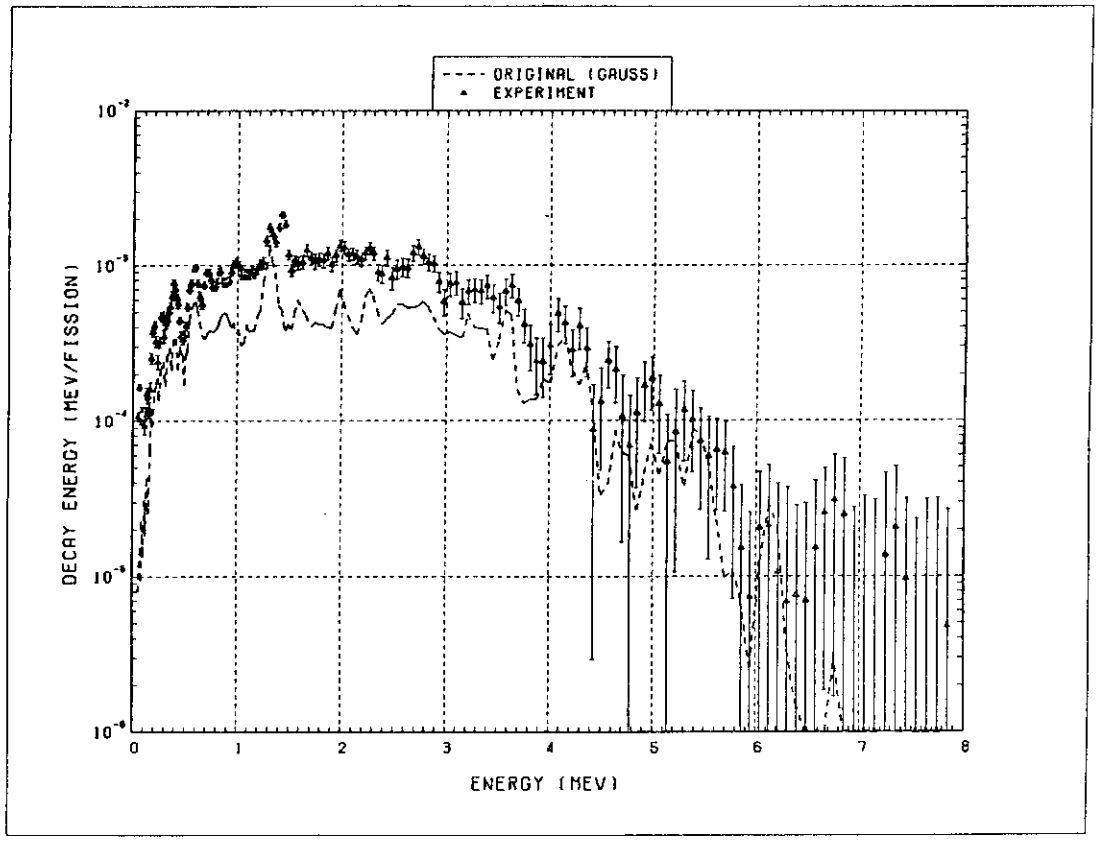

Fig.20 Gamma-ray spectrum at 100.2 sec following ^{239}Pu thermal fission. The notations are the same as in Fig.6.

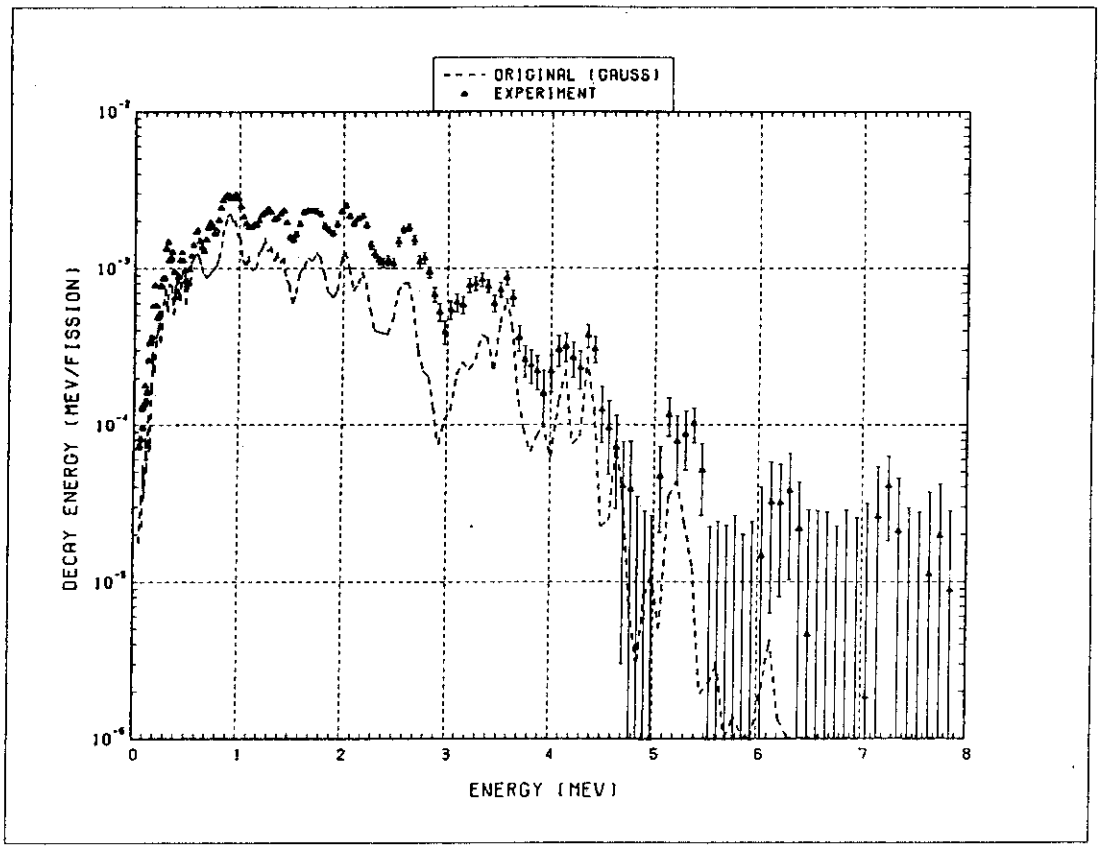

Fig.21 Gamma-ray spectrum at 500.5 sec following ^{239}Pu thermal fission. The notations are the same as in Fig.6.

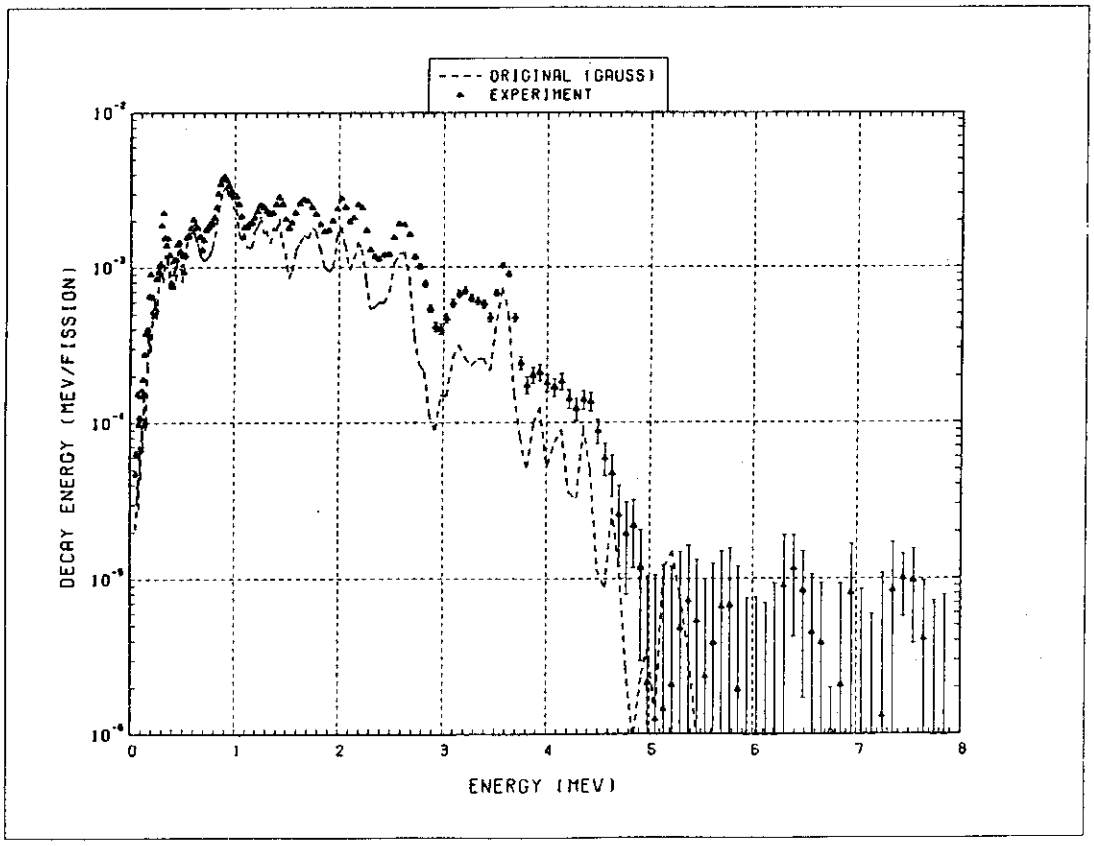

Fig.22 Gamma-ray spectrum at 1000.0 sec following ^{239}Pu thermal fission. The notations are the same as in Fig.6.

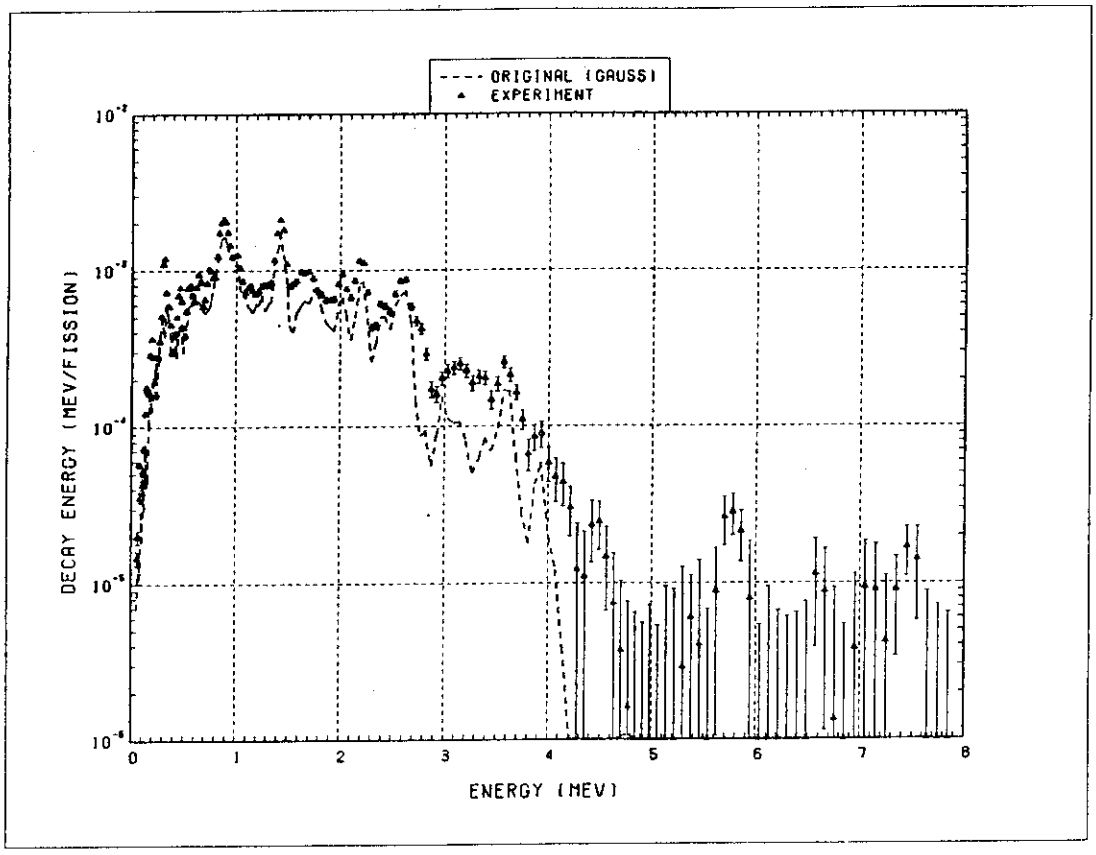

Fig.23 Gamma-ray spectrum at 2750.0 sec following ^{239}Pu thermal fission. The notations are the same as in Fig.6.

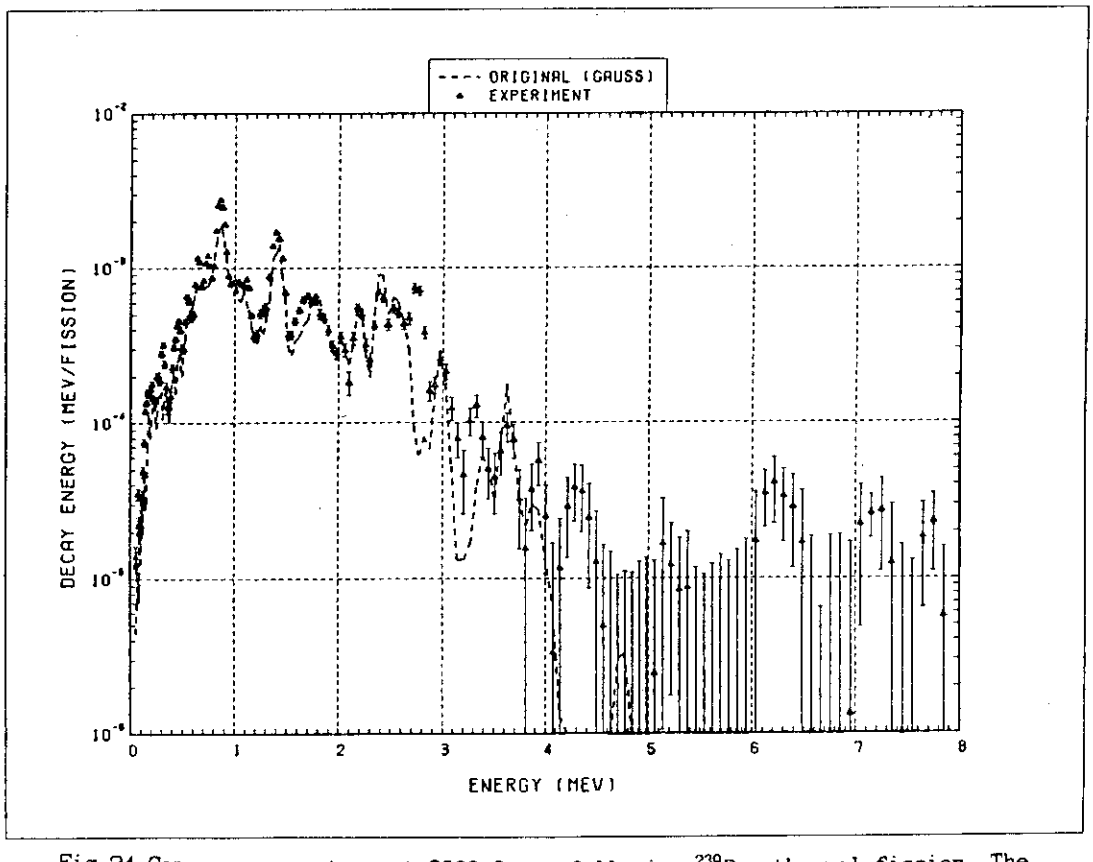

Fig.24 Gamma-ray spectrum at 9000.0 sec following ^{239}Pu thermal fission. The notations are the same as in Fig.6.

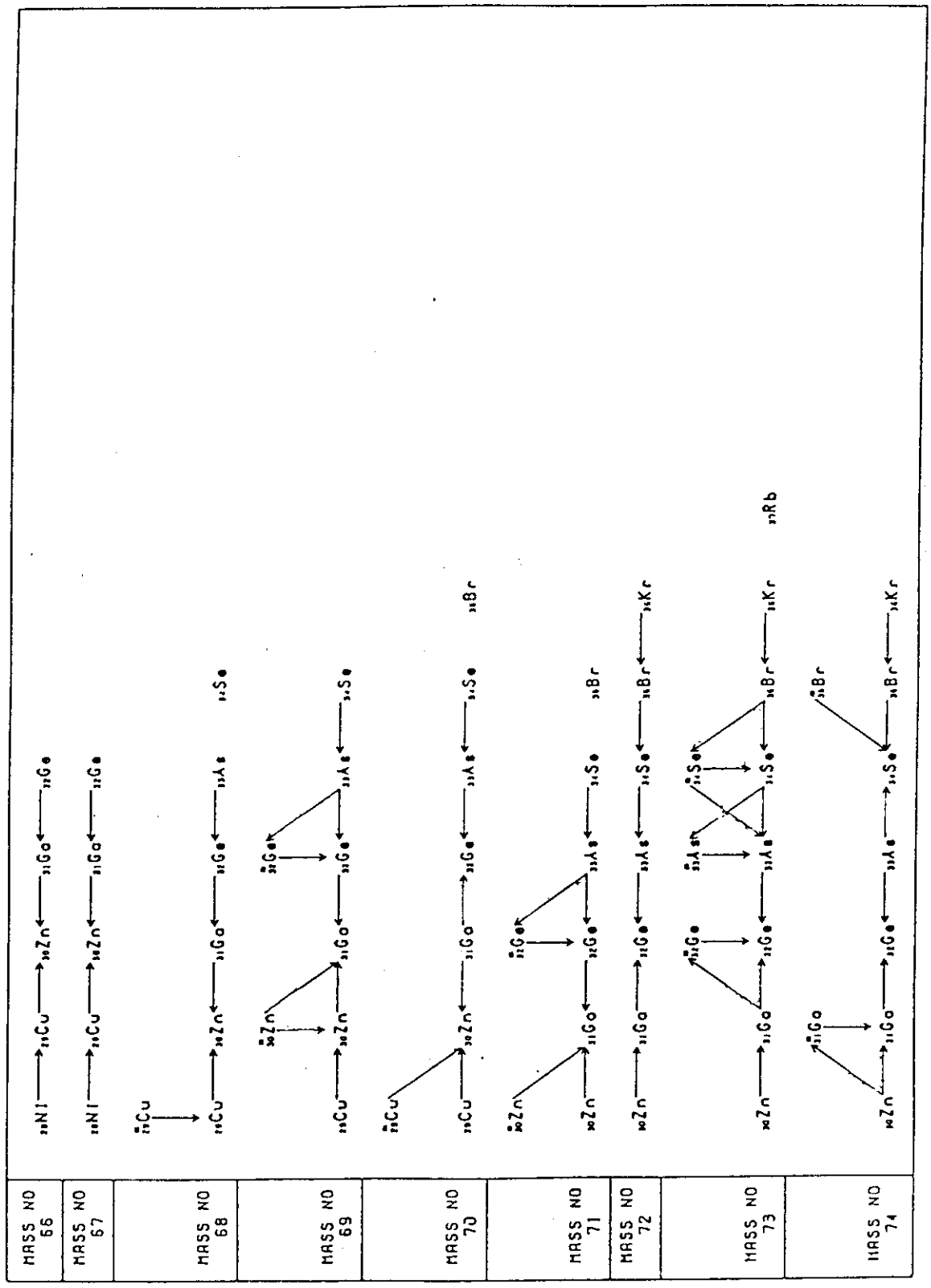

Fig.25 Examples of the decay chains from the ENSDF data.

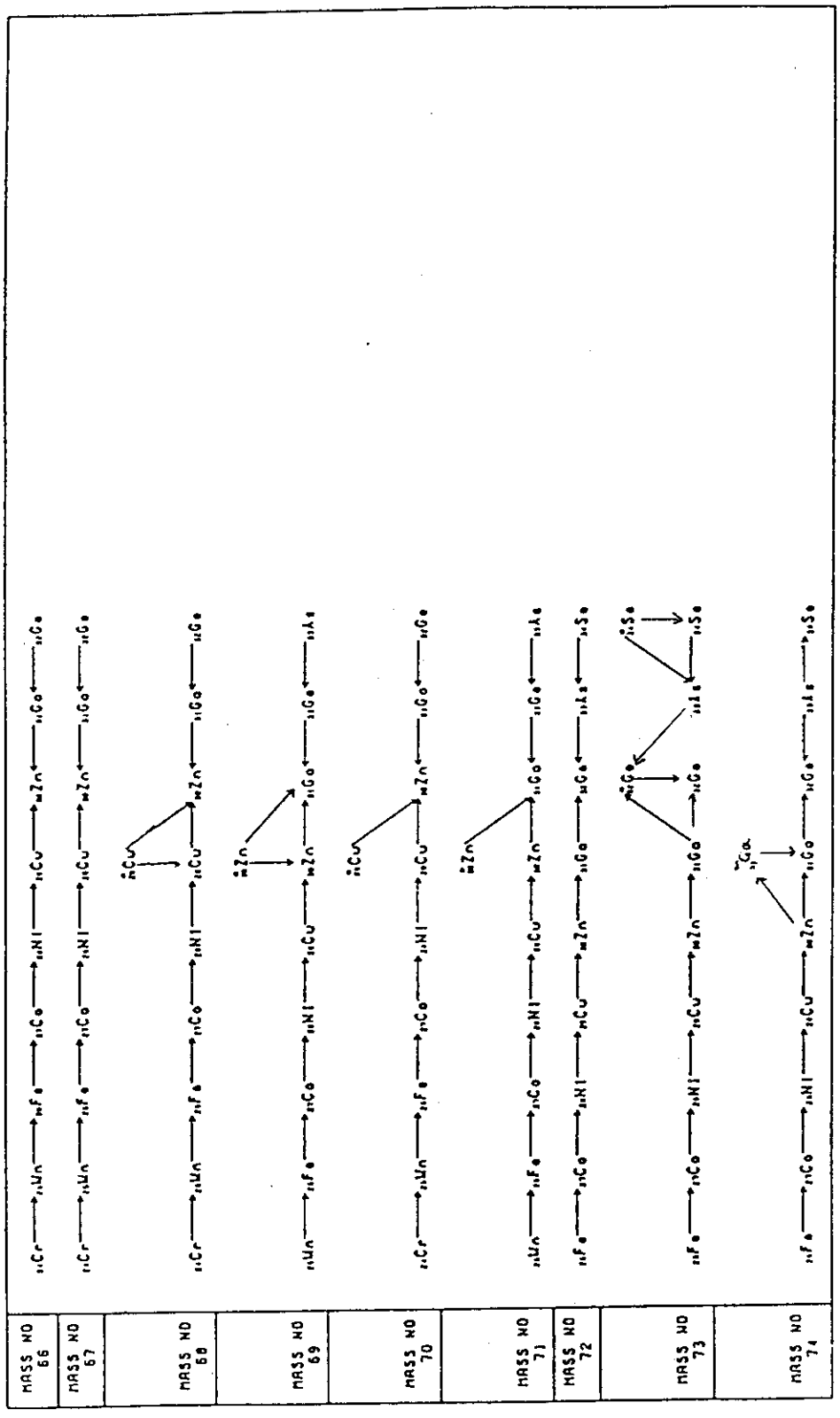

Fig.26 Examples of the decay chains in the JNDC library.

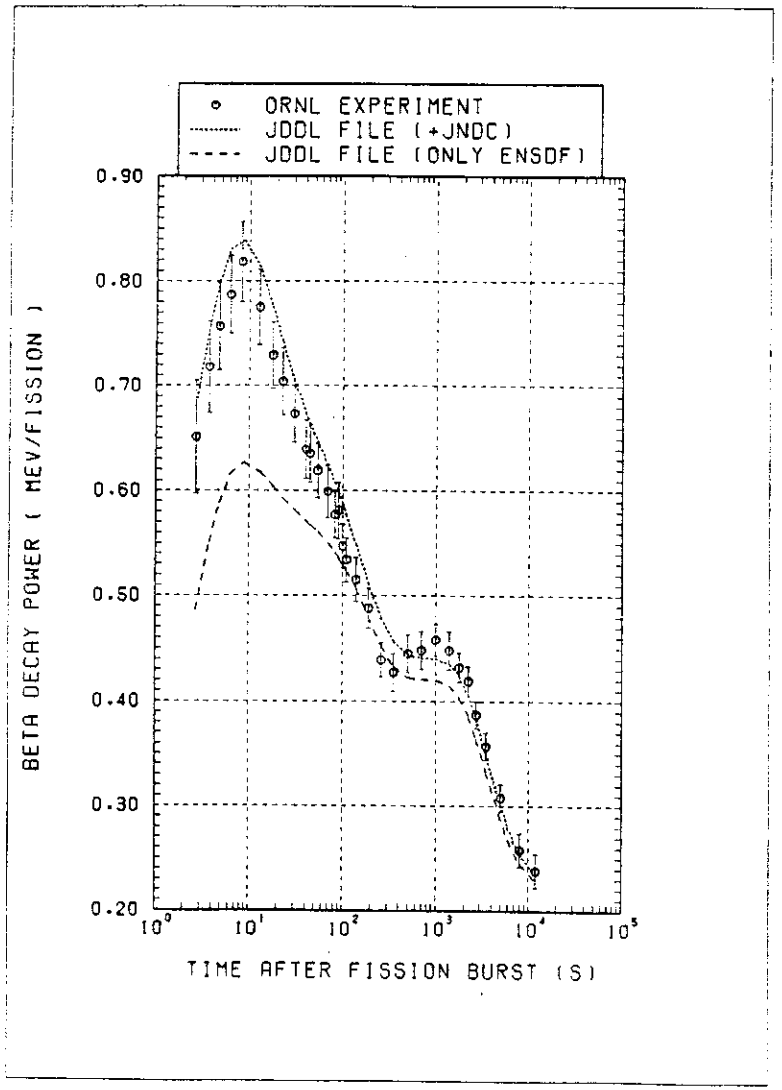

Fig.27 Beta decay power for ^{235}U thermal fission. The data for nuclides with no experimental informations were taken from the JNDC library. The dotted line is a calculated decay power with the revised library. The dashed line is a calculated decay power with the library from only the ENSDF data.

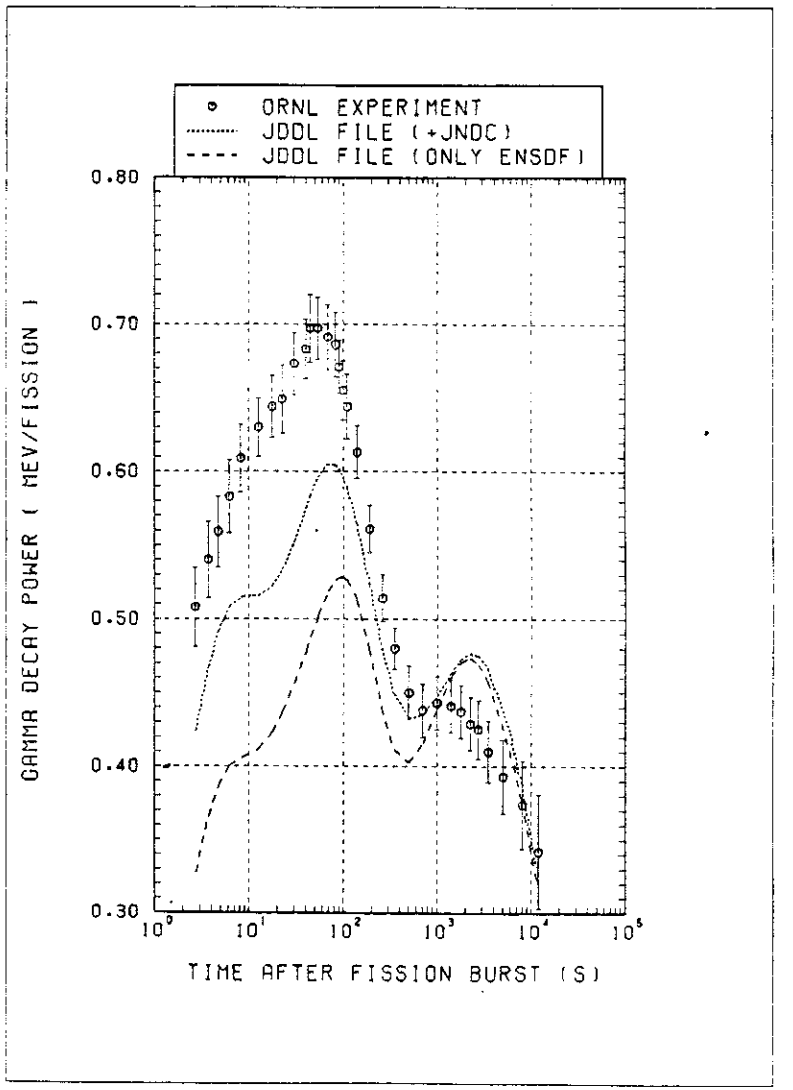

Fig.28 Gamma decay power for ^{235}U thermal fission. The notations are the same as in Fig.27.

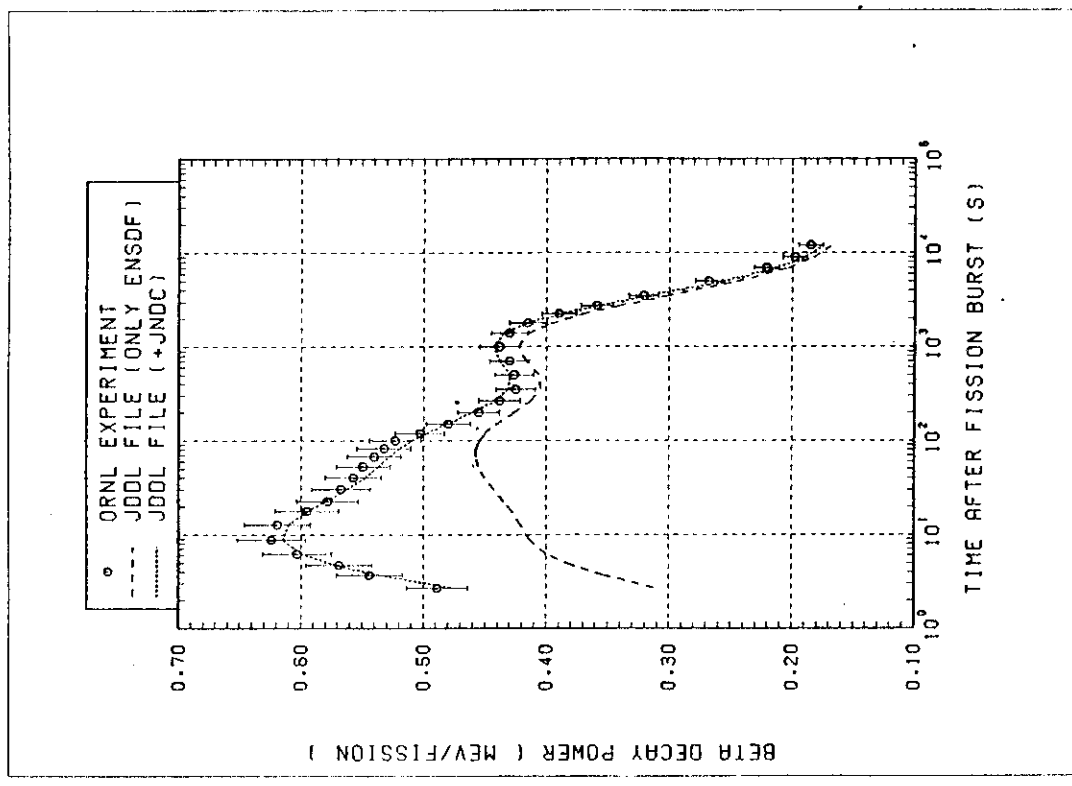

Fig.30 Beta decay power for ^{239}Pu thermal fission. The notations are the same as in Fig.27.

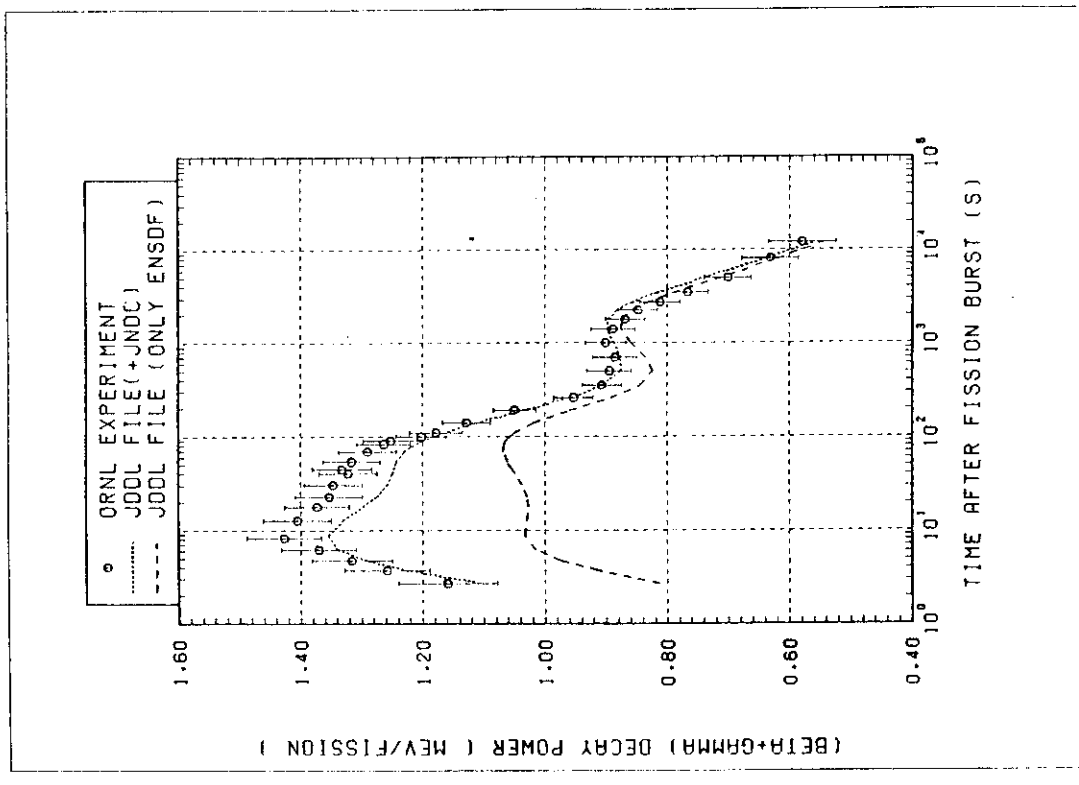

Fig.29 Total decay power for ^{235}U thermal fission. The notations are the same as in Fig.27.

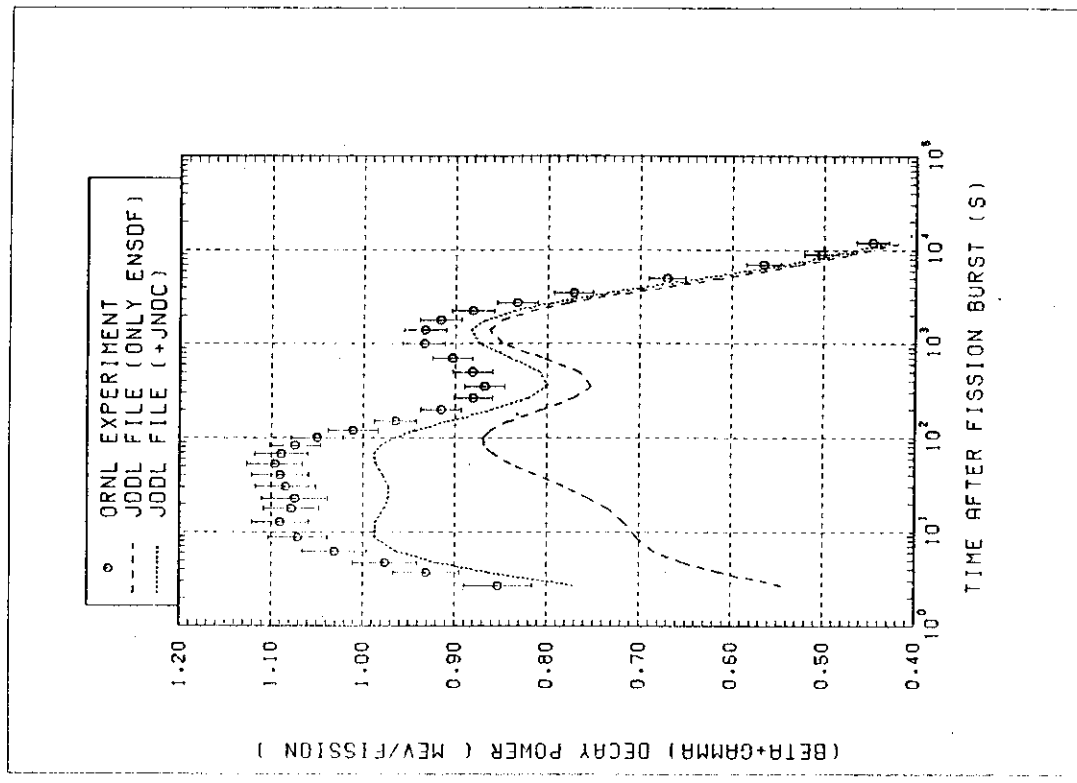

Fig.32 Total decay power for ^{239}Pu thermal fission. The notations are the same as in Fig.27.

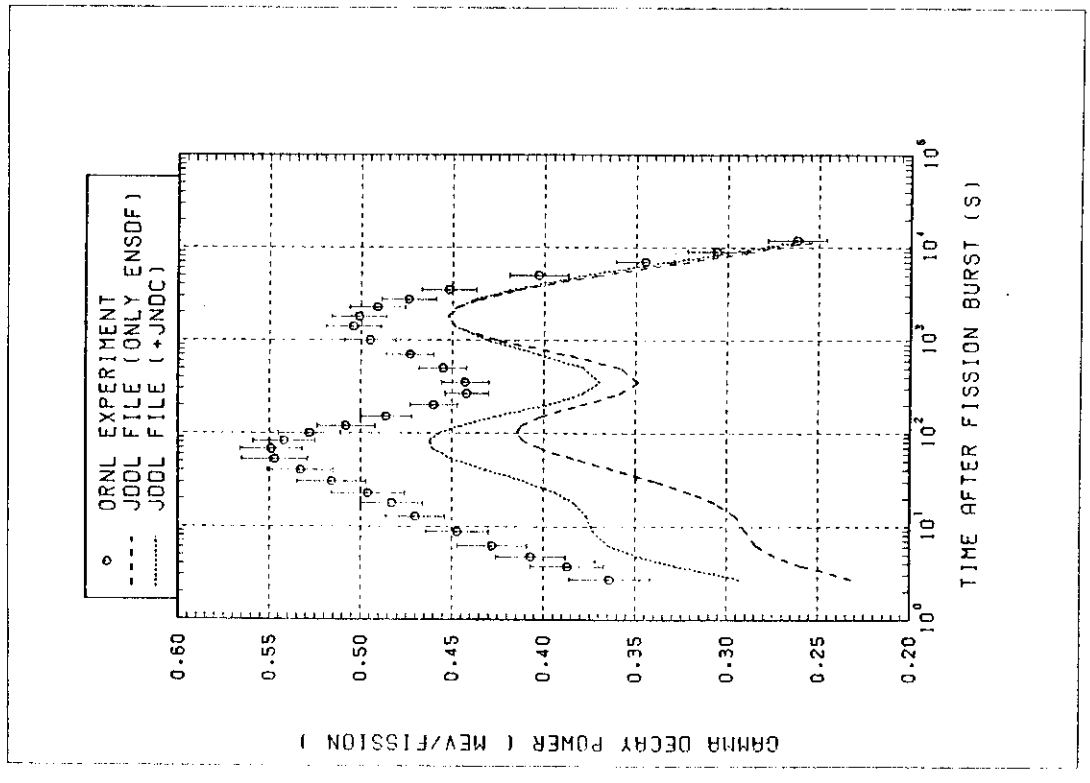

Fig.31 Gamma decay power for ^{239}Pu thermal fission. The notations are the same as in Fig.27.

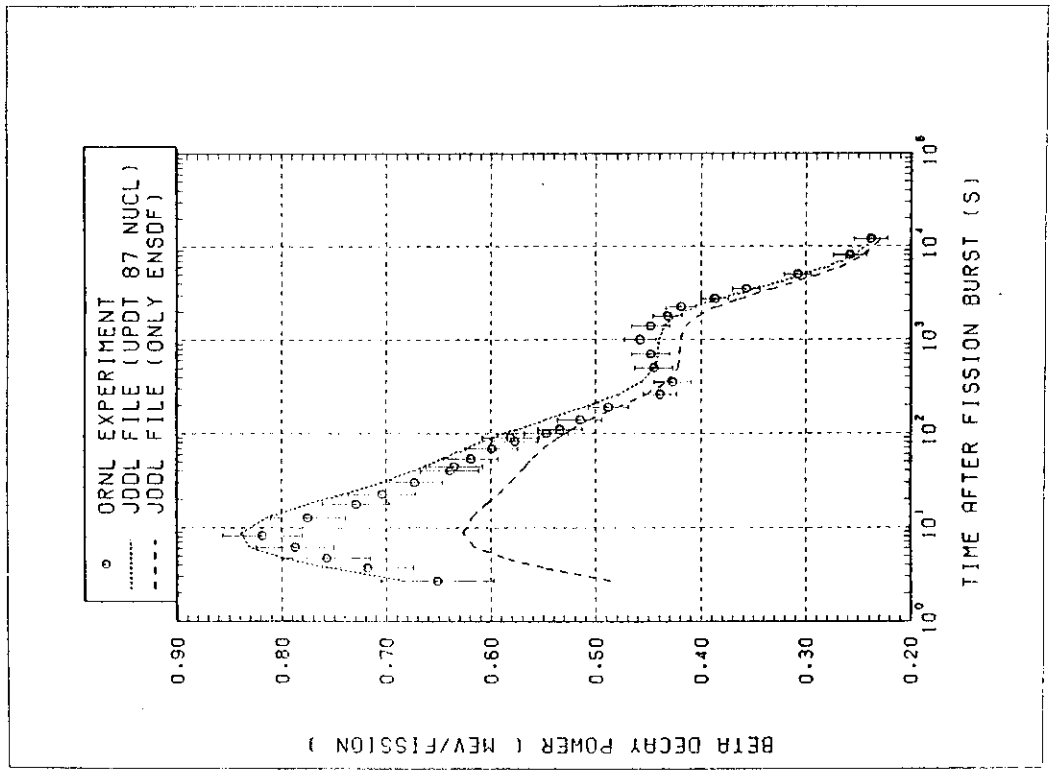

Fig.33 Beta decay power for ^{235}U thermal fission. The data for nuclides with large Q-values are replaced by the estimated values in the JNDC library. The dotted line is a calculated decay power with the JDDL library. The dashed line is a calculated decay power with the library from only the ENSDF data.

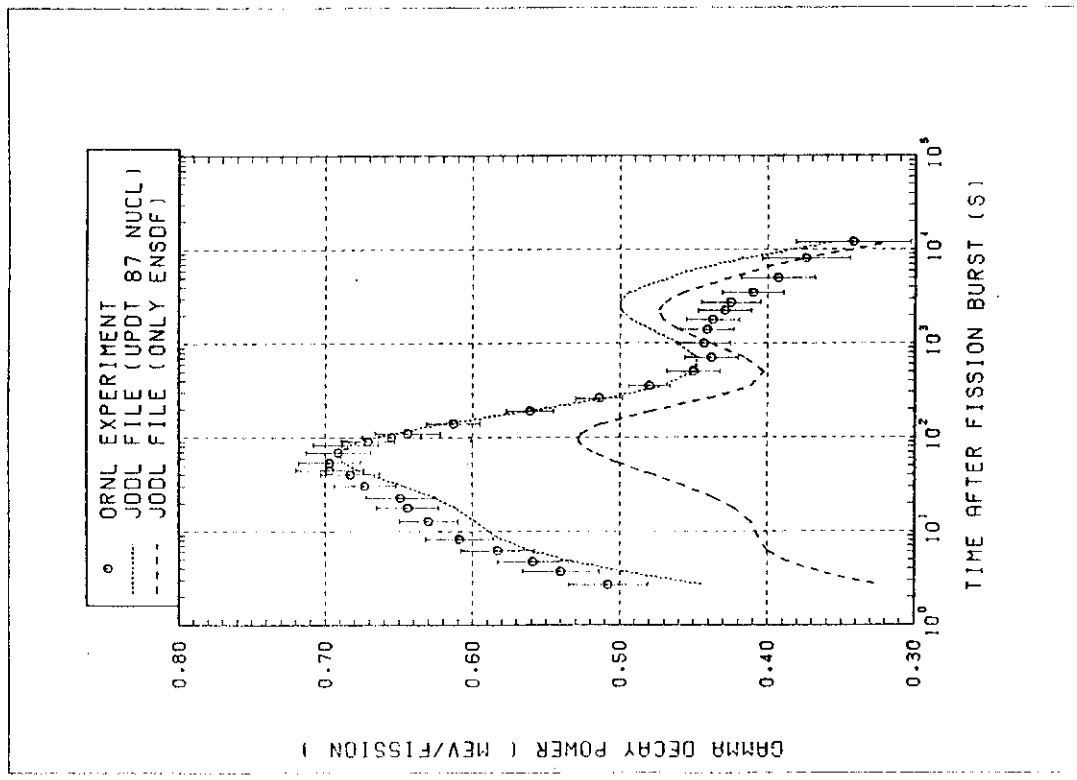

Fig.34 Gamma decay power for ^{235}U thermal fission. The notations are the same as in Fig.33.

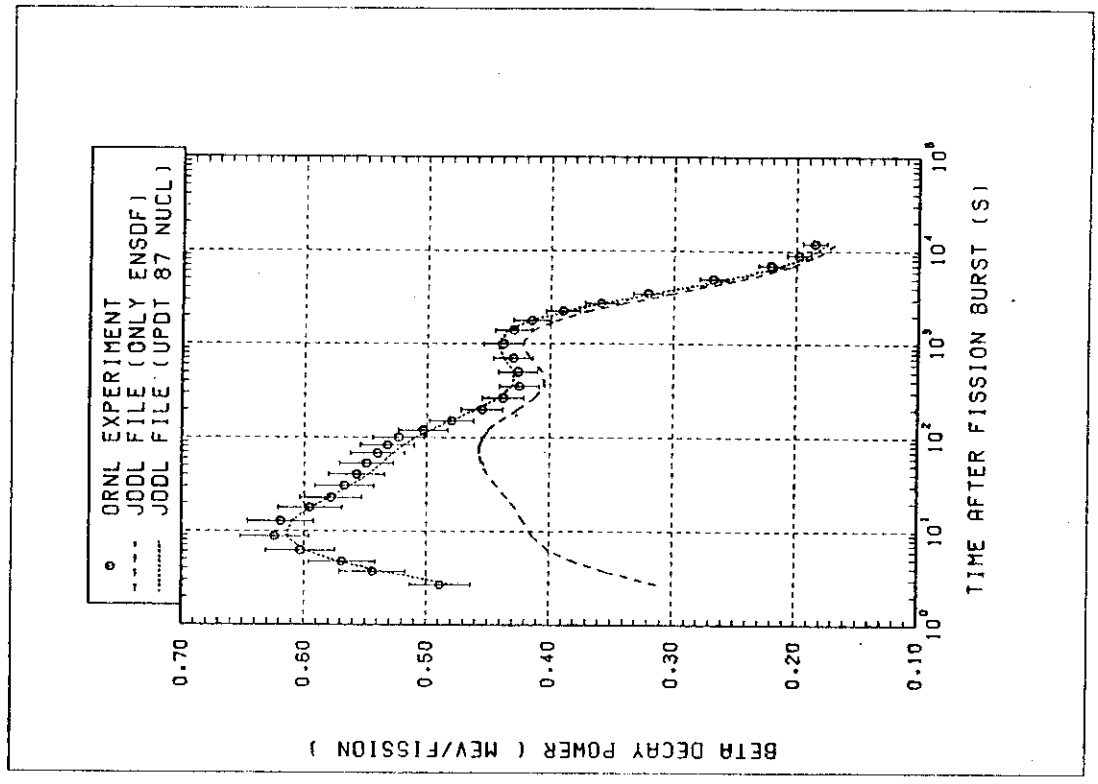

Fig.36 Beta decay power for ^{239}Pu thermal fission. The notations are the same as in Fig.33.

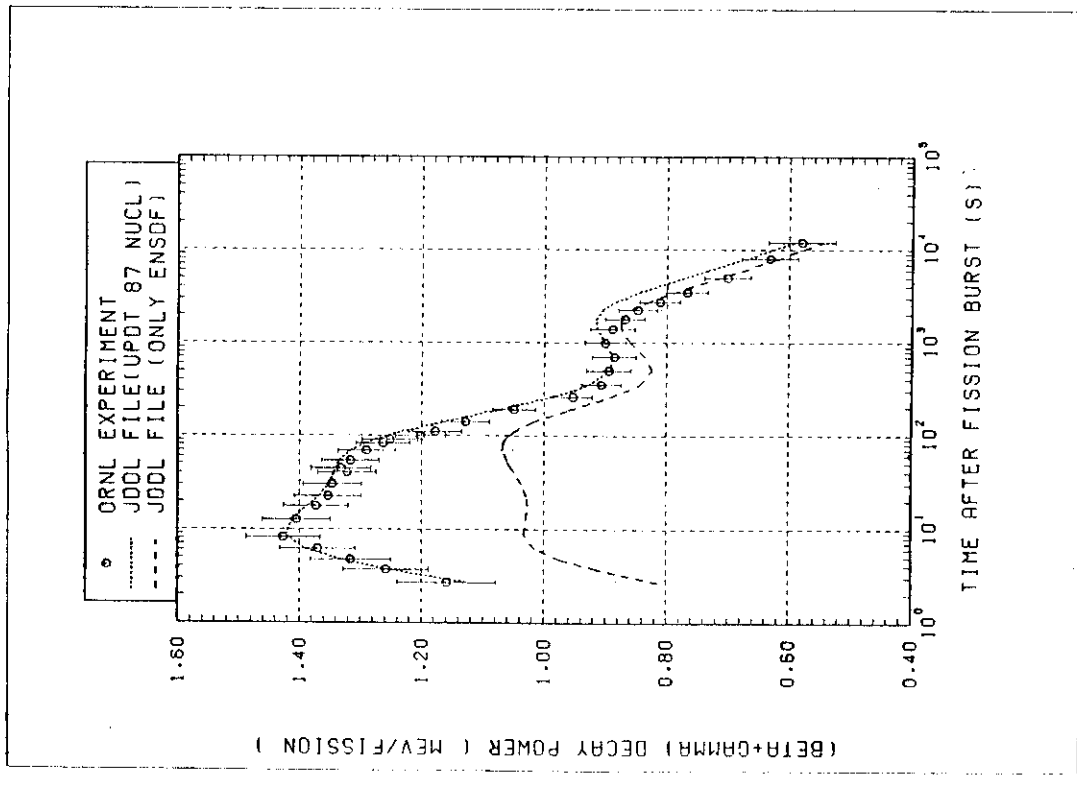

Fig.35 Total decay power for ^{235}U thermal fission. The notations are the same as in Fig.33.

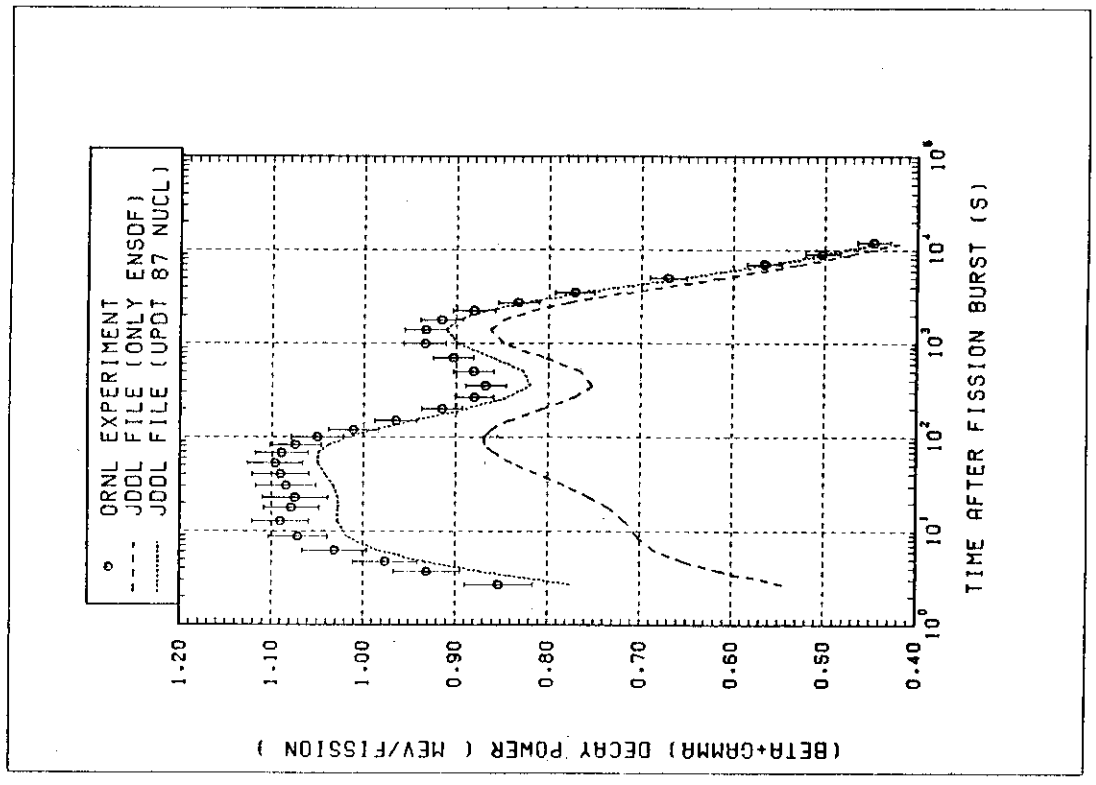

Fig.38 Total decay power for ^{239}Pu thermal fission. The notations are the same as in Fig.6.

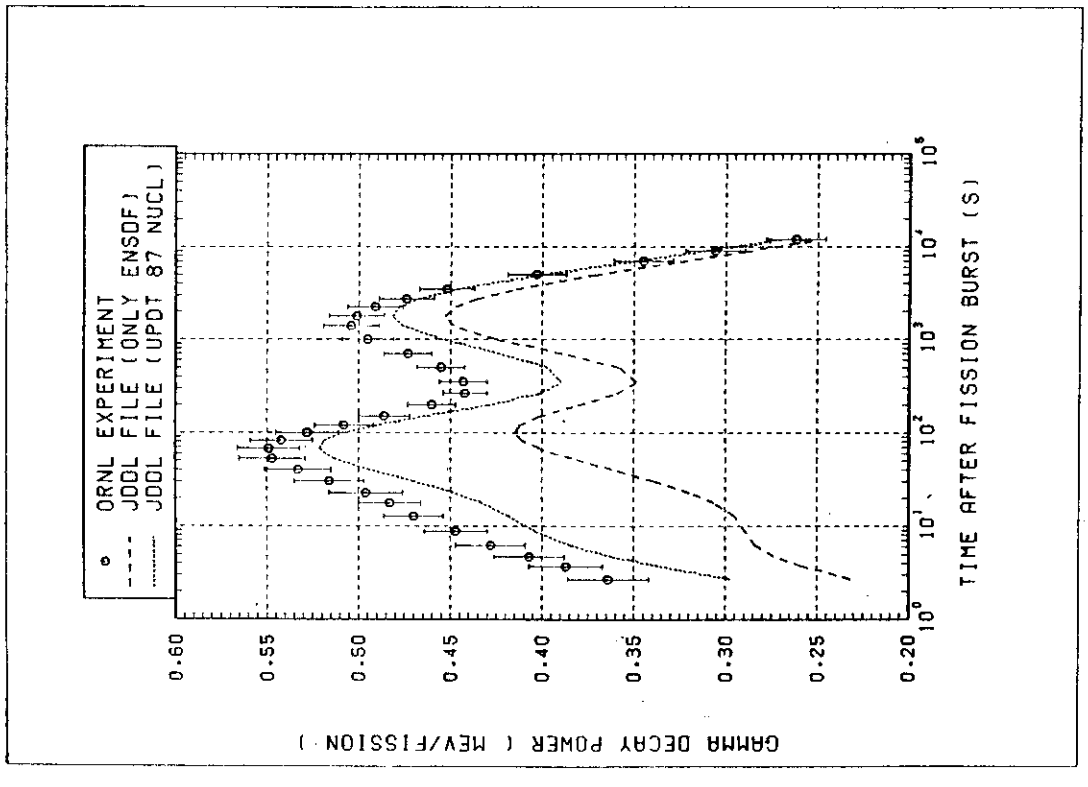

Fig.37 Gamma decay power for ^{239}Pu thermal fission. The notations are the same as in Fig.33.

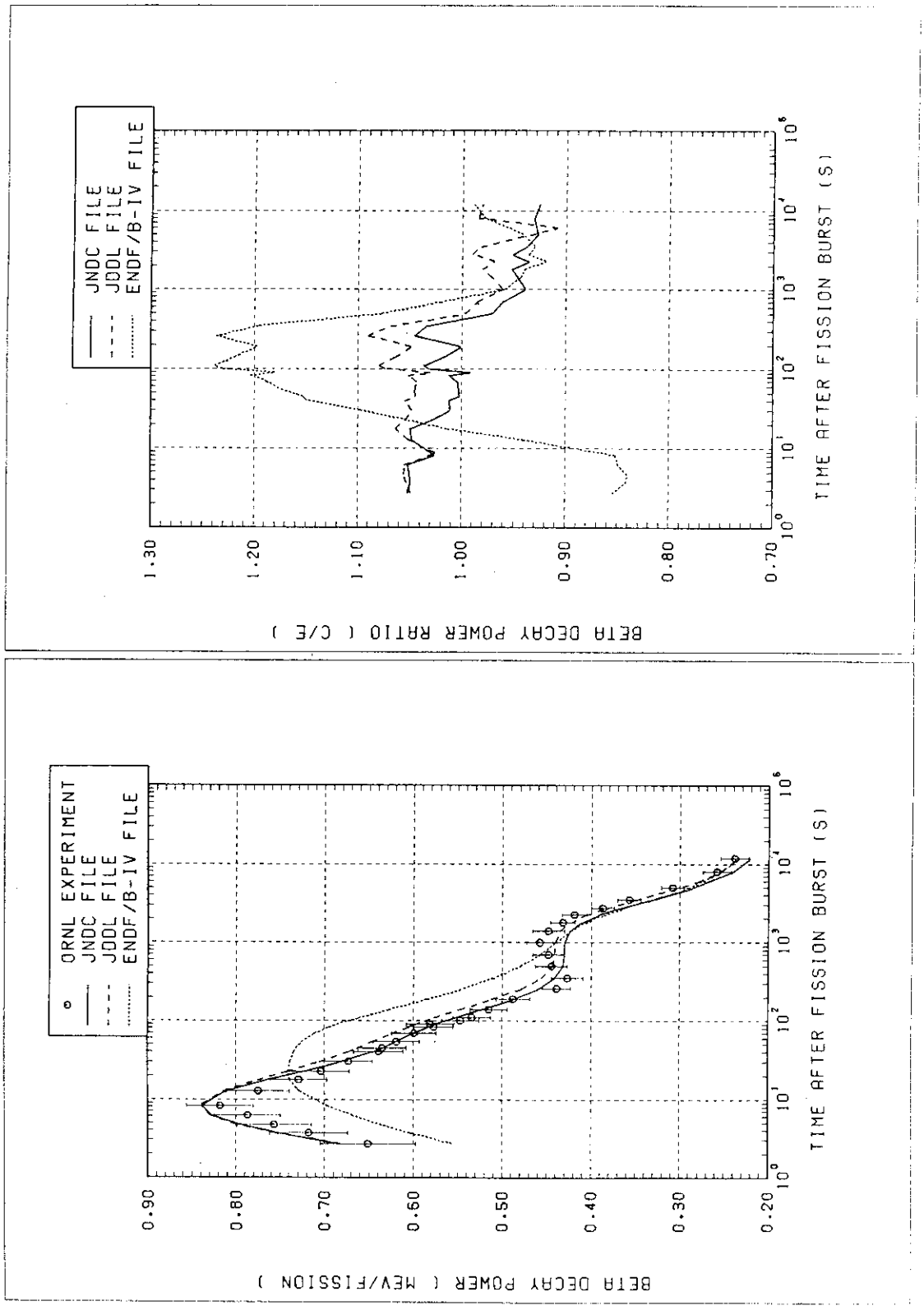

Fig.39 Beta decay power for ^{235}U thermal fission. The present library (JDDL) is compared with the JNDC library and ENDF/B-IV. C/E values (the calculated result divided by the experimental value) are presented in right-hand side.

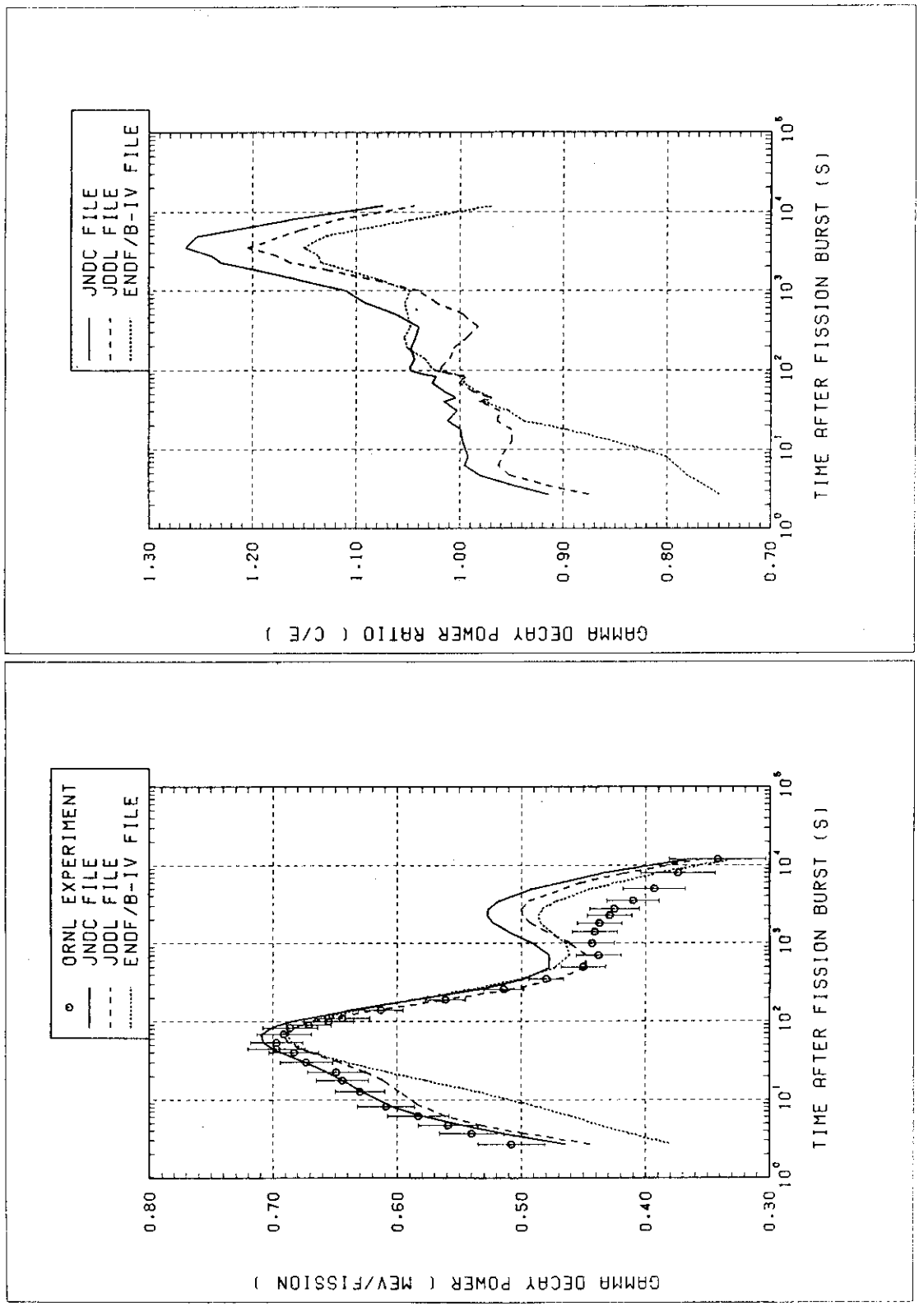

Fig.40 Gamma decay power for ^{235}U thermal fission. The notations are the same as in Fig.39.

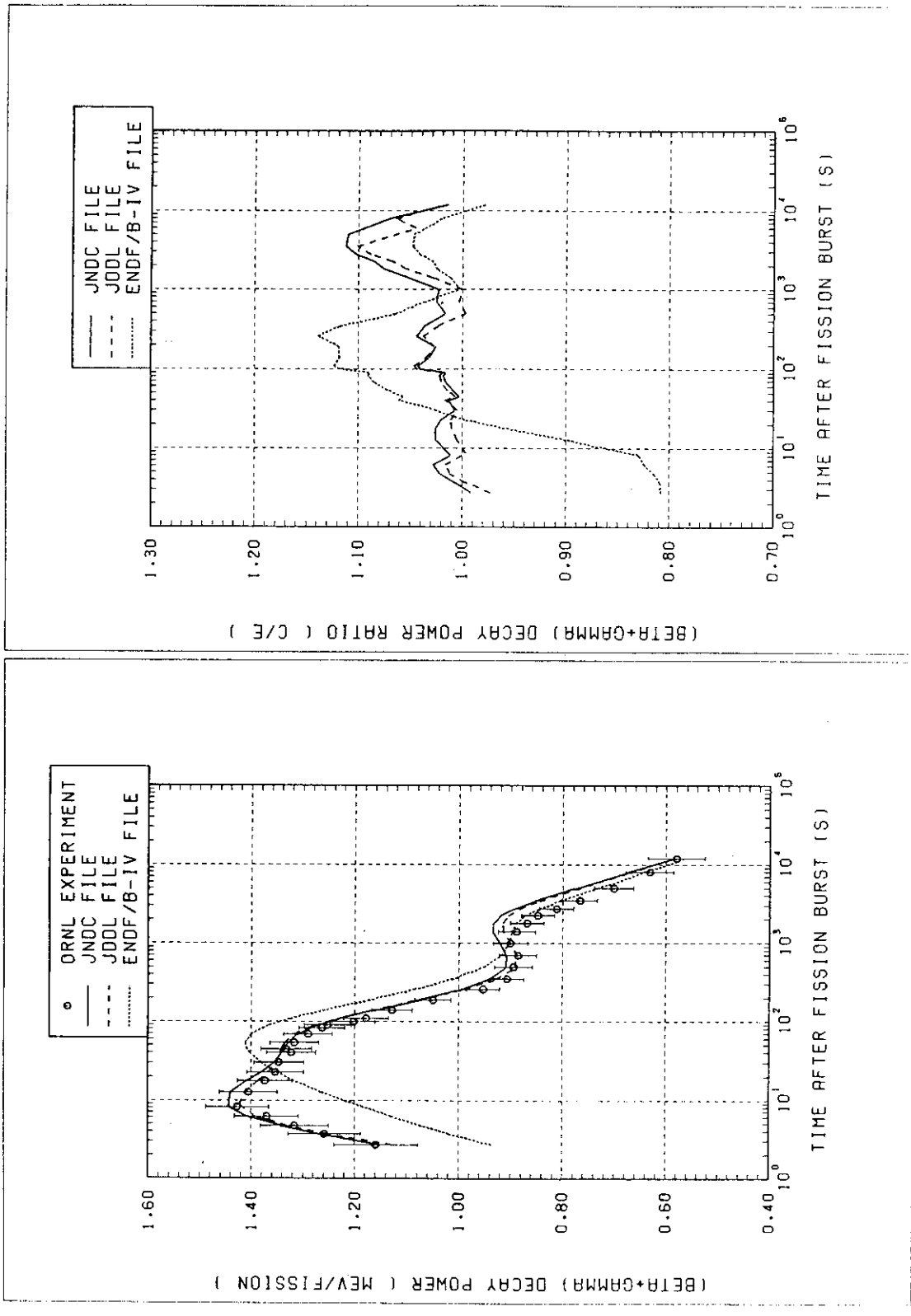

Fig.41 Total decay power for ^{235}U thermal fission. The notations are the same as in Fig.39.

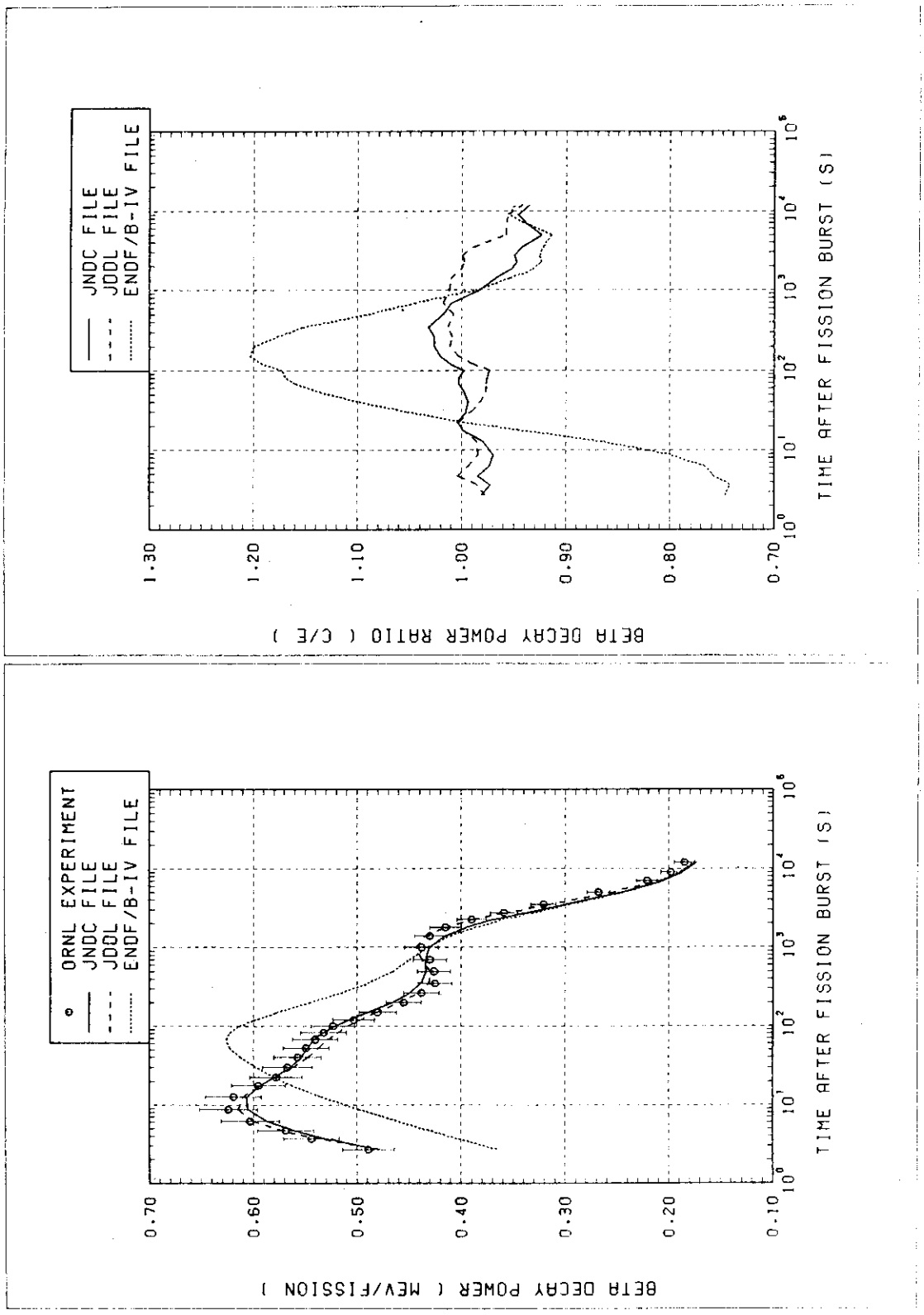

Fig.42 Beta decay power for ^{239}Pu thermal fission. The notations are the same as in Fig.39.

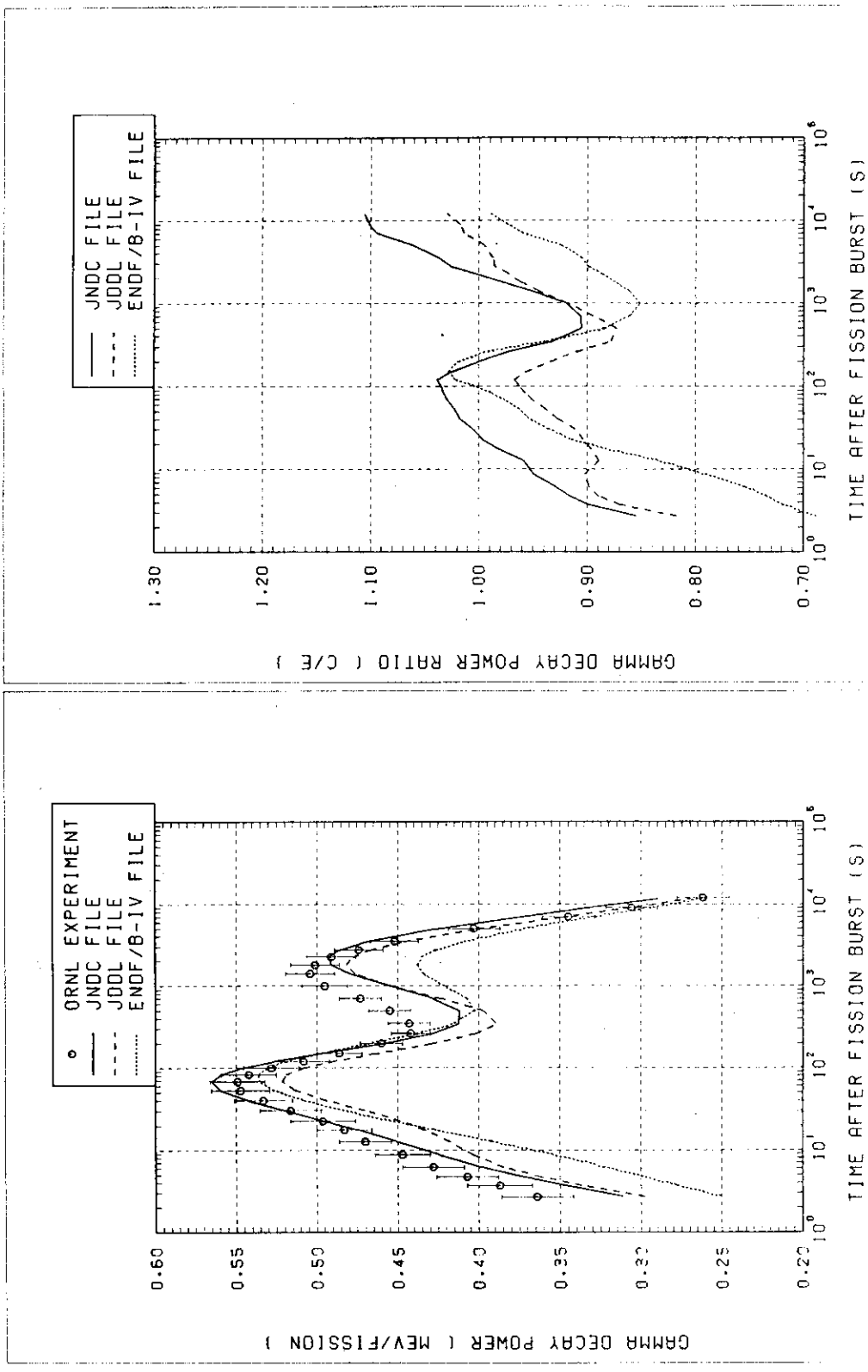

Fig.43 Gamma decay power for ^{239}Pu thermal fission. The notations are the same as in Fig.39.

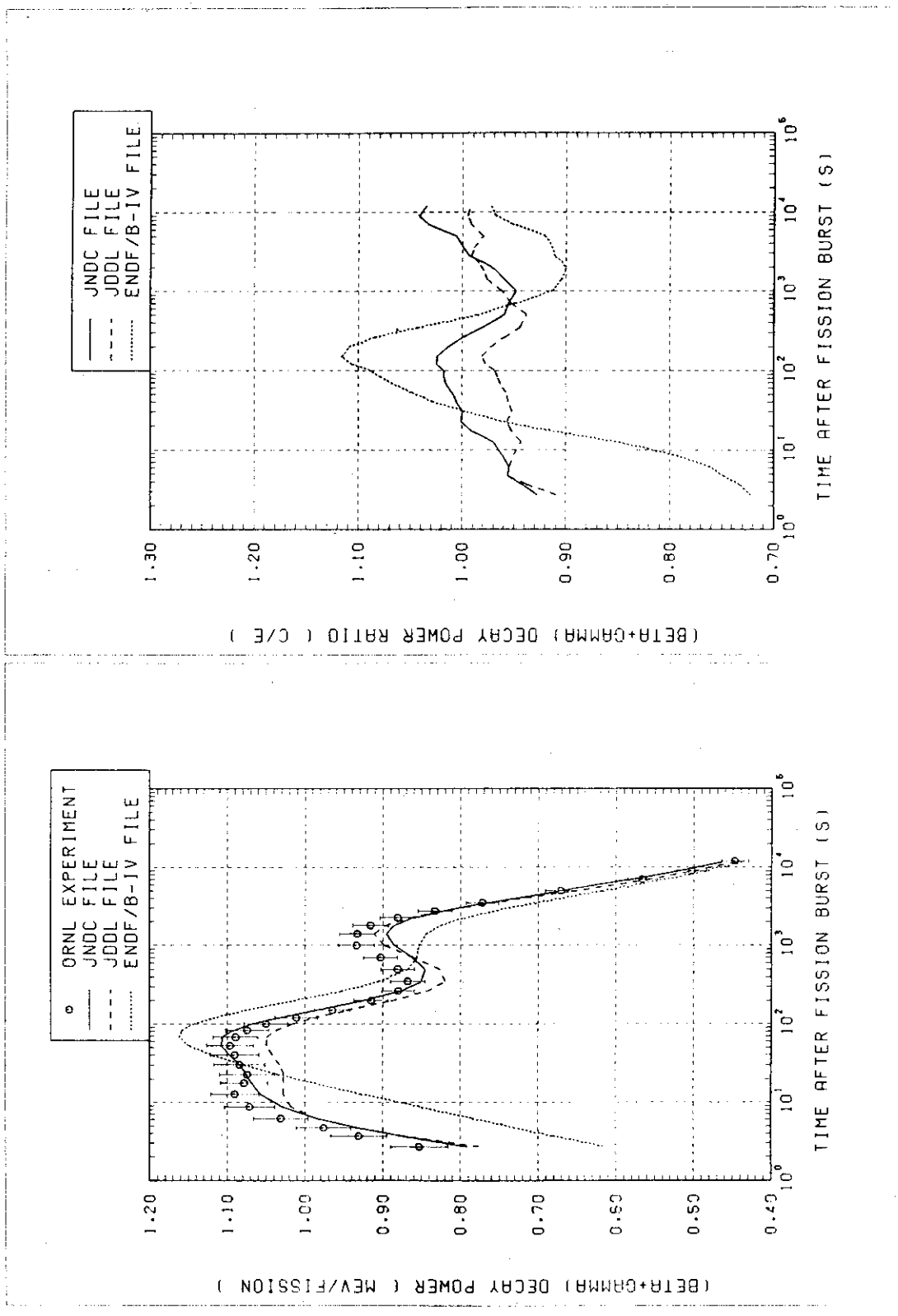

Fig.44 Total decay power for ^{239}Pu thermal fission. The notations are the same as in Fig.39.

Appendix A. Data Description of the ENSDF[3)]

The Evaluated Nuclear Structure Data File (ENSDF)is made up from a collection of "data sets", each of which describes the results of a single experiment or the combined evaluated results of a number of experiments of the same type.

A data set is composed of records ; each record is made up of one or more card images. A data set must begin with an IDENTIFICATION record and must end with an END record (a blank card). Between these two records, there are as many additional records as are needed to describe fully the experiment or the evaluated data set as shown in Table A.1.

Immediately following the IDENTIFICATION record is a group of records which contain information about the entire data set. The NORMALIZATION(N), Q-VALUE(Q), PARENT(P) and general COMMENT(C) records are of this type. The body of a data set is composed of numeric data records which describe the measured or deduced properties of levels, gamma rays, alpha particles, etc.. These records are associated with the level which decays (for GAMMA records) or the level which is populated (for B-, EC or ALPHA records). Thus, each LEVEL record is followed by a group of records describing charged-particle decay into the level and gamma ray decay out of the level.

If a GAMMA record (or ALPHA or B+ or B-) properly belongs in a data set, but it cannot be associated with any paticular level, then the record should be placed in the data set before any level records.

Table A Example of the ENSDF Data Set

```
200AU    200PT B- DECAY                    76HI06                          79NDS     790126
200PT  P 0              0+                 12.5 H    3                      700       SY
200AU  N 0.0134    13            1.0
200AU CN NR          FROM RI(227G)=2.07% BASED ON 200PT-200AU EQUILIBRIUM SOURCE
200AU2CN MEASUREMENTS OF 78HI2W AND THE ASSUMPTION OF 79% B- FEEDING TO 200HG GS
200AU CB IB          THE INTENSITIES WERE CALCULATED ON THE ASSUMPTION THAT ALL
200AU2CB THE GAMMAS ARE M1; THEY SHOULD BE CONSIDERED TENTATIVE
200AU C  198PT(T,P) PRODUCED 200PT, GG COIN GE(LI) (76HI06).
200AU CG M           B- IS EXPECTED TO FEED 0- AND 1- LEVELS IN 200AU;
200AU2CG THEREFORE, MOST MULTIPOLARITIES SHOULD BE PREDOMINANTLY M1
200AU  G  25.21     6    10.2   10 IF M1                          78.0
200AU2 G                  LC=    59.7    %MC=   13.76    %
200AU  G 212.61     29    1.3   5  IF M1                          0.889
200AU2 G KC=   0.730    %LC= 0.1215    %MC= 0.0281    %N+=0.00883    %
200AU  G 218.17     21    2.5   6  IF M1                          0.827
200AU2 G KC=   0.680    %LC= 0.1130    %MC= 0.0261    %N+=0.00821    %
200AU  G 251.46     22    4.8   8  IF M1                          0.558
200AU2 G KC=   0.459    %LC= 0.0761    %MC=0.01760    %N+=0.00551    %
200AU  L 0              1-
200AU  B                19      8                  6.8719
200AU2 B EAV=  218.47    %
200AU  L 59.98          (0,1,2)-
200AU  B                 1      LT                 8.01GT                          ?
200AU2 B EAV=  197.09    %
200AU  G  60.00     4   172     10 IF M1                          6.01
200AU2 G                  LC=    4.60    %MC=   1.069    %N+=   0.236    %
200AU  L 76.21          (0,1,2)-
200AU  B                46      5                  6.31 5
200AU2 B EAV=  191.37    %
200AU  G  76.20     5 1000        IF M1                          2.98
200AU2 G                  LC=   2.286    %MC=   0.530    %N+= 0.1674    %
200AU  L 103.65
200AU  B                 8.2    10                 7.00 6
200AU2 B EAV=  181.76    %
200AU  G  27.48     10    2.9    9  IF M1                          60.4
200AU2 G                  LC=    46.2    %MC=   10.66    %
200AU  G  43.67     4    59.9    24 IF M1                         15.31
200AU2 G                  LC=   11.69    %MC=    2.72    %
200AU  G 103.60     9    76.7    41 IF M1                          6.81
200AU2 G KC=    5.59    %LC=  0.937    %MC= 0.2179    %N+= 0.0694    %
200AU  L 166.00                                                                  ?
200AU  B                 0.48   20                 8.0719
200AU2 B EAV=  160.26    %
200AU  G 166.00     20   38     4  IF M1                          1.777
200AU2 G KC=   1.458    %LC= 0.2438    %MC= 0.0564    %N+=0.01786    %
200AU  L 239.54          (0,1)-
200AU  B                12.9    15                 6.42 6
200AU2 B EAV=  135.51    %
200AU  G 135.94     15  242     14 IF M1                          3.14
200AU2 G KC=    2.57    %LC=  0.431    %MC= 0.0998    %N+= 0.0317    %
200AU  G 179.40     19    3.5   6  IF M1                          1.424
200AU2 G KC=   1.169    %LC= 0.1958    %MC= 0.0453    %N+=0.01431    %
200AU  G 239.56     16    5.9   8  IF M1                          0.638
200AU2 G KC=   0.525    %LC= 0.0871    %MC=0.02013    %N+=0.00631    %
200AU  L 243.58
200AU  B                 0.3    LT                 8.05GT
200AU2 B EAV=  134.17    %
200AU  G 140.09     21    5.2   23 IF M1                          2.88
200AU2 G KC=   2.363    %LC=  0.395    %MC= 0.0915    %N+= 0.0291    %
200AU  G 167.37     21   28     4  IF M1                          1.735
200AU2 G KC=   1.425    %LC= 0.2382    %MC= 0.0551    %N+=0.01745    %
```